Universität Stuttgart

Deutsches SOFIA Institut

SOFIA‘s Invisible Universe

An infrared kit manual for schools

with experiments you can perform yourself

Produced by the

Deutsches SOFIA Institut (DSI)

University of Stuttgart

in cooperation with the

House of Astronomy (HdA)

and

Wissenschaft in die Schulen (WIS)

Dr. Cecilia Scorza (DSI & HdA)

Dr. Olaf Fischer (HdA & WIS)

Translation: Antje Lischke-Weis (DSI) and Hassnat Ahmad

Edition of the English Version: Dana Backman (USRA)

A look in the kit - 1

1 - Webcam, infrared emitter

2 - Prism and NIR (near-infrared) indication cards

3 - Active speaker and solar cell

4 - Infrared lamp and aluminum plate (matte)

5 - Remote control and model of water molecule

6 - Hand spectroscope, rubber balls, and black plastic bag

A look in the kit - 2

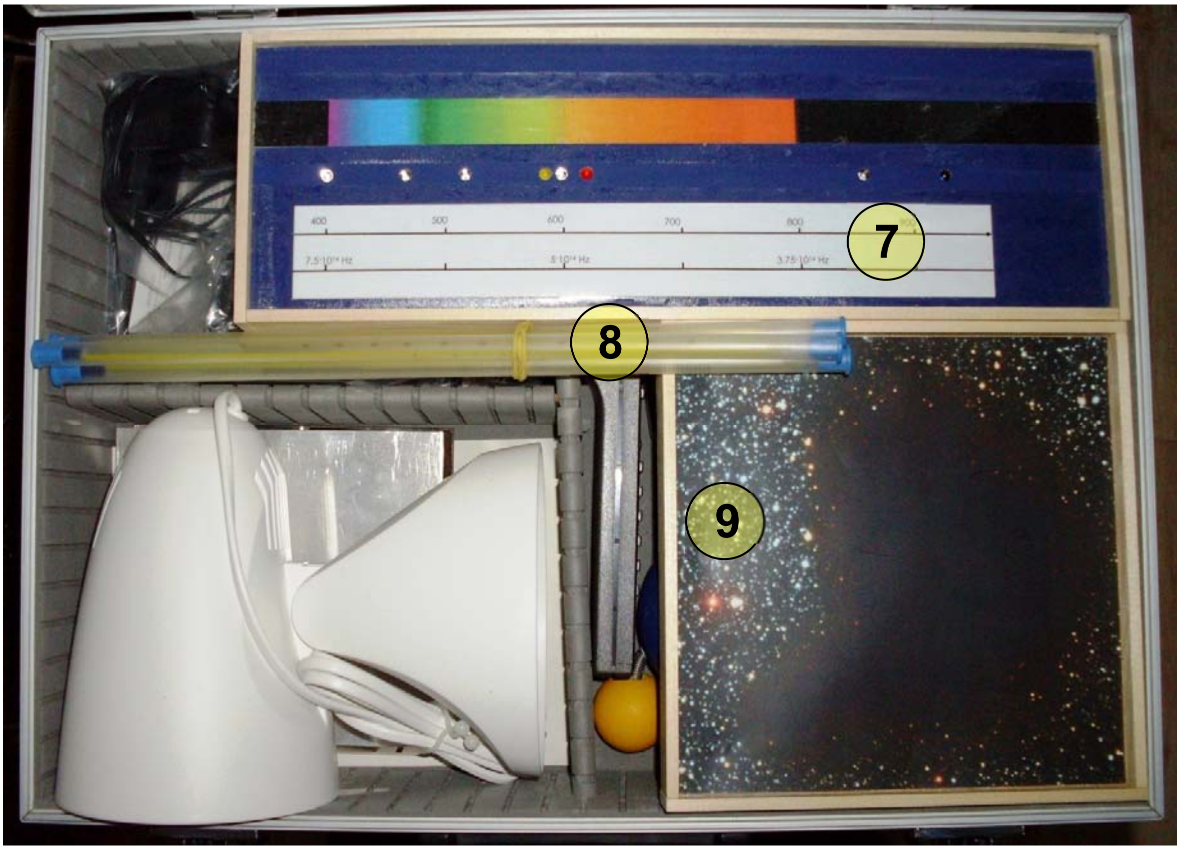

7 - 'Spectrino' model

8 - Three thermometers for the Herschel experiment

9 - Dark nebula model

Color-coding in this manual

This manual contains basic theoretical background regarding infrared radiation, customized for middle school and high school students. For clarity and in order to locate the astronomical topics and activities for easy implementation in the classroom, the following color-coding is used throughout this manual:

Applications in astronomy

Activities and experiments

Contents

1. SOFIA, an airborne observatory

In May 2010 a new chapter in the history of astronomy and aeronautics was opened: the largest airborne observatory, containing a reflecting telescope with an effective diameter of 2.5 meters (100 inches), made its first observations. SOFIA stands for **S**tratospheric **O**bservatory **f**or **I**nfrared **A**stronomy), and gives astronomers opportunities to investigate:

- Surfaces of comets, asteroids, moons, and planets in our solar system;
- Sizes and atmospheric composition of exoplanets;
- Origin and evolution of stars in our Galaxy and other galaxies;
- Influences of black holes on the nuclei of galaxies including ours.

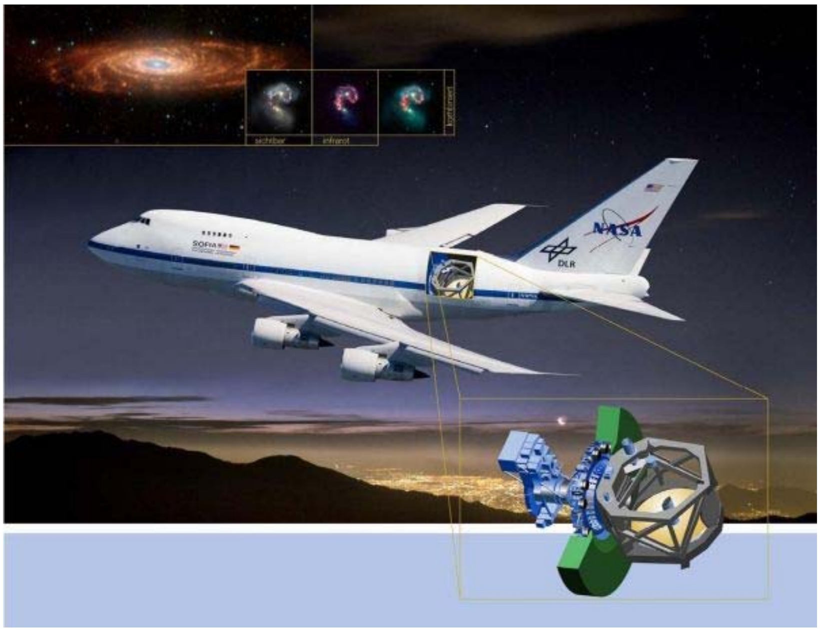

SOFIA, the **S**tratospheric **O**bservatory **f**or **I**nfrared **A**stronomy is a joint project of the Deutsches Zentrum für Luft- und Raumfahrt e.V. (DLR; German Aerospace Center, grant: 50OK0901 and 50OK1301) and the National Aeronautics and Space Administration (NASA). SOFIA is funded on behalf of DLR by the Federal Ministry of Economics and Energy based on legislation by the German Parliament, the state of Baden-Württemberg, and the Universität Stuttgart. SOFIA scientific operations are coordinated in Germany by the Deutsches SOFIA Institut (DSI; German SOFIA Institute) at the Universität Stuttgart, and in the U.S. by the Universities Space Research Association (USRA) SOFIA Science Center at NASA's Ames Research Center in Northern California.

Infrared radiation (IR) from celestial sources is difficult to detect on Earth's due to the absorption of IR by water vapor in the atmosphere. Therefore SOFIA climbs to altitudes of more than 13 kilometers (43,000 feet) to make observations above most of this water vapor.

This book is about infrared radiation. Specific phenomena of this radiation in astronomy are shown in relation to ordinary down-to-Earth observations of infrared radiation. Starting with the discovery of IR, an informative overlook is given of the physical characteristics of IR as well as of the interaction of IR with matter. Different sources and receivers will be used to learn about IR. This infrared kit manual for schools, with experiments you can perform yourself, provides an opportunity for you to implement infrared astronomy into your school and school district's physical science and physics curricula.

1.1 The discovery of infrared radiation (IR)

As in many cases in the history of science, infrared radiation was discovered by chance. Friedrich Wilhelm Herschel (1738-1822), a German musician from Hannover, devoted his spare time to astronomy and worked on building large telescopes. In England in summer of 1800, he studied the spectrum of sunlight, not knowing that he was on the verge of a great discovery. He was interested in the relationship between color and the heat emitted by the Sun in each spectral range. For this reason, he let sunlight fall through a slit on a prism and measured the respective temperatures in the light of each color.

The story goes that Herschel left his measuring apparatus unattended for a short tea break. When he returned, the position of the Sun in the sky and accordingly the spectrum relative to the thermometers had shifted. To his surprise, he discovered that beyond the red spectral region, where there is nothing more to be seen by eye, the thermometer indicated the highest temperature. Herschel repeated this experiment several times and came to the conclusion that there must be a form of radiation invisible to the human eye. Without knowing it, with this discovery Herschel had opened a new huge window in astronomy. (image from univie.ac.at)

Shortly after Herschel's discovery, astronomers wanted to observe the Moon, planets, asteroids, and even comets in the infrared (IR). This wish, however, remained unfulfilled for a long time, since there were no better detectors for infrared radiation than thermometers.

After Herschel's discovery the idea quickly arose to investigate infrared radiation from the moon, planets, asteroids, and comets. Because the only infrared detectors available at the time, thermometers, were not very sensitive, this vision could not be realized for more than a century.

An important step was the development of the germanium bolometer by Frank J. Low in 1961 that was sensitive to the full range of infrared radiation. Its function is based on the change of electrical resistance of a germanium semiconductor when exposed to infrared radiation. If a constant voltage is applied the change of resistance across a bit of germanium can be detected precisely and thereby the amount of incident infrared radiation determined (photograph courtesy the Astronomical Society of the Pacific).

Expectations were high; one could now investigate the infrared universe! However, a big barrier to observation of infrared radiation from celestial sources is its strong absorption by the water vapor in Earth's atmosphere. Even under a clear sky and with relatively low humidity, most infrared radiation is blocked from reaching Earth's surface. Additional problems are thermal radiation from the instrument and from the atmosphere. So, the next step was to cool the germanium detector to very low temperature and bring the telescope as high as possible in the Earth's atmosphere.

To this end, in 1960 the Dutch-American astronomer Gerard Kuiper built an infrared telescope onboard a NASA research aircraft. This aircraft had been designed originally to investigate the Earth's atmosphere; the newly installed telescope looked through an aircraft window to observe infrared radiation from the universe for the first time (NASA photograph archive).

Using this first airborne infrared observatory that was named Galileo, the clouds of Venus were characterized; they are mainly composed of sulphuric acid instead of water vapor as had previously been assumed. Investigation of Saturn's rings showed that they contain frozen water. Tragically, the Galileo observatory was destroyed in a collision with another plane during landing at NASA Ames's Moffett Field in northern California; the scientists and pilots onboard lost their lives.

At this time a second airborne infrared observatory was already under construction. To have a replacement available more quickly a window of a Learjet was removed and a 30 cm (approx. 12 inch) telescope was installed to make astronomical infrared observations.

The conditions for the astronomers onboard were very cramped and they had to wear pressure suits plus respirator masks. However, their investigations were very successful. They discovered that the radiation emitted from Jupiter and Saturn in the infrared range is more than what they absorb from the Sun, which means those planets must have internal sources of energy (NASA photograph archive).

For the first time the interior of interstellar clouds could be observed, structure that are hidden for observations at visible wavelengths due to strong absorption by interstellar dust.

A big improvement was made in 1974 with NASA's Kuiper Airborne Observatory (KAO). A Lockheed C141 Starlifter cargo jet aircraft was modified to carry a 91.5 cm (36 inch) telescope mounted inside an opening in front of the wing. Because of the much larger telescope diameter then the Learjet observatory, a better and deeper view into the universe was possible (NASA photography archive).

Some of the main discoveries made with KAO are the rings of Uranus, and the thin methane atmosphere of Pluto. It could be verified that comets contains water and the distribution of water and other organic molecules in the interstellar media was observed. In 1995 KAO was retired and was replaced be the **S**tratospheric **O**bservatory **F**or **I**nfrared **A**stronomy – SOFIA.

KAO and SOFIA on the airfield at the Ames Research Center (photograph of NASA archive).

Activity 1: Perform your own Herschel experiment

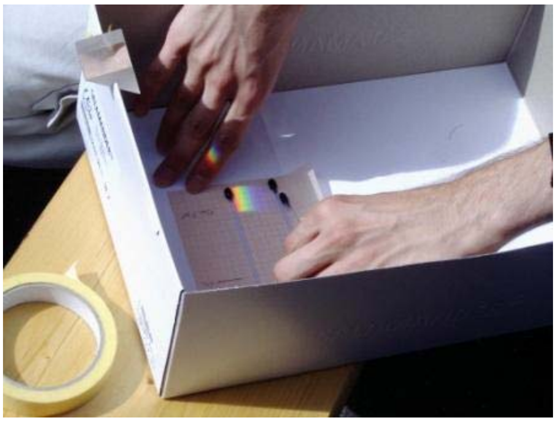

For the Herschel experiment, you will need:

- A glass prism,
- Matte black paint,
- Three alcohol thermometers,
- A clock, and
- A cardboard box.

For the thermometers to better absorb the Sun’s infrared radiation, paint the liquid reservoir of the thermometers with black paint. Now, measure the ambient temperature in the shade.

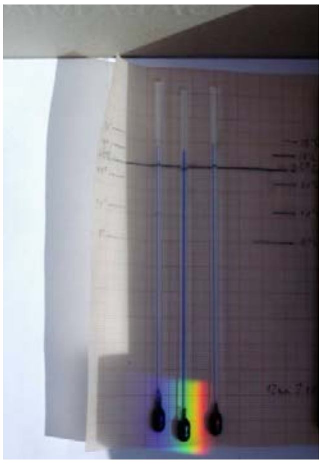

Attach the prism on the edge of the cardboard box and generate a spectrum as broad as possible. Place a thermometer in the blue, green, and infrared areas, respectively. Measure the temperatures at intervals of one minute for an overall period of 5 minutes and write down the results. (Also write down the initial temperature, which is the ambient temperature.) Each of the three thermometers shows an increase in temperature of a few degrees C, the largest increase being detected in the infrared area.

Food for thought: The Sun its most intense energy in the yellow-green spectral range. Try to find explanations why this fact apparently does not come into play in the experiment.

Physics information box

The refractive index of a medium is different for different wavelengths (referred to ‘dispersion’). This makes it possible to decompose white light into a spectrum (prism). The dispersion of prisms does not occur linearly; they stretch towards blue and gather towards red.

Likewise, the absorption capability (of the thermometer liquid) depends on the wavelength.

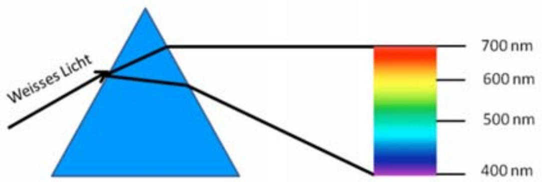

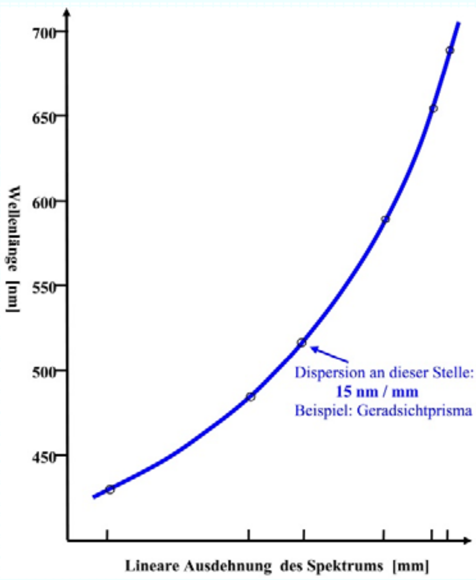

Time (min)	Temperature (°C) Blue	Temperature (°C) Green	Temperature (°C) IR
Initial			
1 min			
2 min			
3 min			
4 min			
5 min			

Table of measured values for the Herschel experiment

Interpretation of the results and reasons for any apparent contradictions:

2. The nature of light and infrared radiation

2.1 Light as a wave phenomenon

Visible light, as well as infrared radiation that is invisible to us, are only two parts of the radiation emitted by the Sun. Light can be described as a wave, as an electromagnetic waves, to be more specific. The important parameters for characterizing a wave are its *wavelength* λ (the distance between two wave crests or troughs), its *frequency f* that tells us how many wave crests or troughs arrive per second, and its amplitude A, which quantifies the height of a wave crest 'above' the zero line. The shorter the wavelength, the more waves arrive per second, and correspondingly the higher the frequency (see figure below). Conversely, the frequency becomes smaller as the wavelength increases. The frequency f can be calculated from the wavelength λ and the wave propagation velocity c using the relation $f = c / \lambda$ that applies to any type of wave. The propagation velocity c for light in vacuum is about 300 000 km/s.

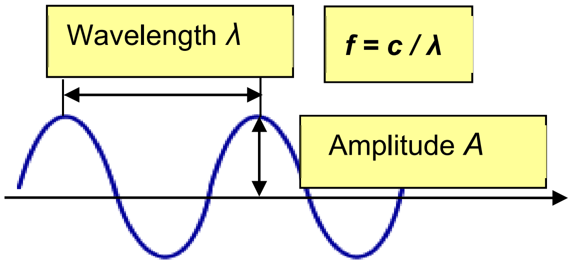

The colorful spectrum of sunlight is caused by electromagnetic waves with different frequencies. The waves in the violet range have a higher frequency than the ones in the blue range, which in turn have higher frequencies than the waves in the red range. Beyond the red region on one side and the violet region on the other, the electromagnetic spectrum extends to shorter (ultraviolet, X-rays, and gamma rays) and longer (infrared, microwave, radio waves) wavelengths, respectively. We are not able to perceive these electromagnetic waves with our eyes, because the 'detectors' of our eyes (the photoreceptors in the retina) are not sensitive in these regions of the electromagnetic spectrum.

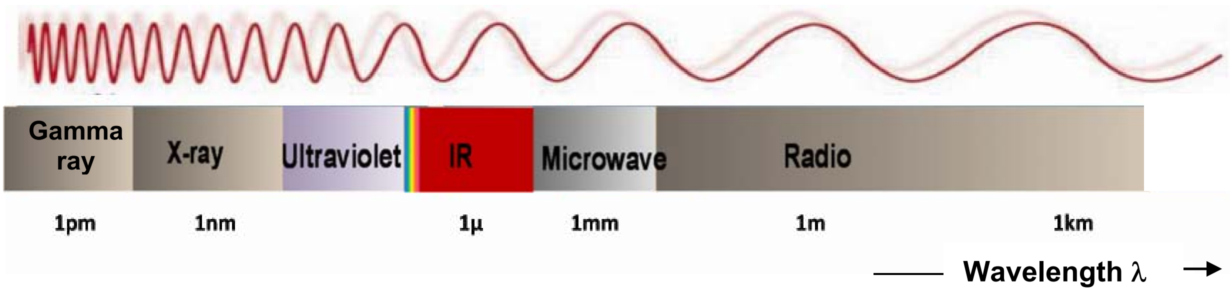

Electromagnetic waves transport energy. The radiant energy of a wave depends on the frequency and the amplitude of the wave. The higher the frequency and amplitude, the more energy the wave can transport:

$$E \sim f; \quad E \sim A^2$$

Gamma rays (with very high frequencies) are the most energetic form of electromagnetic radiation, whereas radio waves (with very low frequencies) have the lowest energy. **Important**: The energy of electromagnetic radiation is transported in quanta (i.e. energy portions of the quantity $E = h \cdot f$); h is a constant called Planck's constant.

2.2 The laws of thermal radiation

Herschel discovered infrared radiation in 1800. The physical explanation of the radiation of heated bodies, however, was not achieved until the formulation of the blackbody model (Gustav Kirchhoff, 1860).

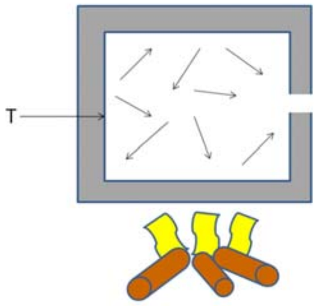

The blackbody is a hypothetical body, which in practice can be approximated by a cavity radiator (see figure). Its absorption capacity and emissivity is 100% for all wavelengths. The radiation of the blackbody depends only on temperature and is independent of all other material properties. Thus, the blackbody is an ideal reference. The thermal radiation of a blackbody is determined by Planck's law and its corollaries the Stefan-Boltzmann law and Wien's displacement law.

Planck's law (1) describes the distribution of the intensity of electromagnetic energy emitted by a blackbody at a temperature T as a function of the wavelength λ or the frequency f. The curves in the P-λ-diagram (see below) are called Planck curves.

(1) $$P(f,T) = \underbrace{\left(8\pi \cdot f^2 / \mathrm{c}^3\right)}_{\text{Number of waves in the interval}} \cdot \underbrace{\left(\mathrm{h} \cdot f\right)}_{\text{Energy of a “wave packet“}} \cdot \underbrace{\left(\left(1 / e^{\mathrm{h}f/\mathrm{k}T}\right) - 1\right)}_{\text{Distribution function}}$$

f…Frequency
c…Light propagation velocity in vacuum
h…Planck’s constant
k…Boltzmann’s constant

The **Stefan-Boltzmann law** quantifies the radiant energy of a blackbody at a temperature T per unit time and per unit area (2) or by a total area A (3), respectively.

(2) $S = \sigma \cdot T^4$

(3) $P = \sigma \cdot A \cdot T^4$

S…Power density
σ…Stefan-Boltzmann constant
T…Temperature
P…Power
A…Area

Wien's displacement law (4) states that the cooler a body is, the more the radiation maximum is shifted towards longer wavelengths. A body at room temperature radiates most strongly in the infrared (more precisely, in the MIR).

(4) $T \cdot \lambda = \text{constant}$

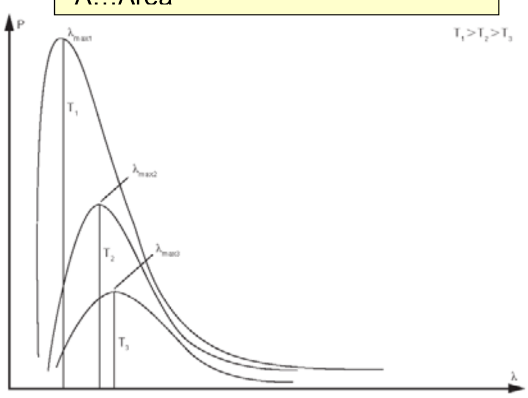

2.3 Infrared radiation (IR) as part of the electromagnetic spectrum

The infrared region lies adjacent to the red end of the visible light spectrum. Bodies with temperatures between 2000 K (1700 °C) and 10 K (-263 °C) are sources of infrared radiation, i.e. all the objects that we know from our neighborhood are infrared radiators. Humans with body temperature of 37 °C radiate at most at a wavelength of about 10 microns. Interstellar dust clouds are one of the coldest types of objects that exist. They have temperatures between 20 and 50 K (for example, the Horsehead Nebula in the constellation Orion). Image VLT, VLT KUEYEN with FORS2).

Infrared radiation is usually considered as divided into three wavelength ranges: near-infrared (NIR), mid-infrared (MIR) and far-infrared (FIR).

NIR 0,8 to 5 microns
MIR 5 to 30 microns
FIR 30 to 350 microns
submm 350 to 1000 microns

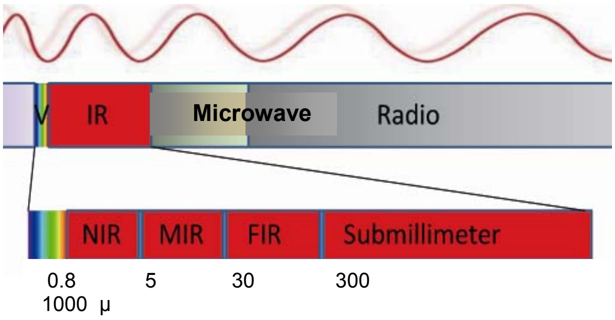

Often, infrared radiation is confused with heat radiation. However, heat radiation is *only a part* of the infrared range. Heat radiation corresponds to the MIR range and is the radiation that is generated normally by atomic and molecular motion at Terrestrial temperatures. Radiation towards shorter wavelengths, such as NIR, visual light, ultraviolet, and X-rays, generally is produced by electron transitions.

The division of the IR into three ranges goes back to the sensitivity of infrared detectors and the infrared transparency of Earth's atmosphere. In particular, water vapor in the air absorbs FIR radiation effectively. It only partly allows MIR radiation of the Sun and of other celestial bodies to pass through. The same is true of carbon dioxide.

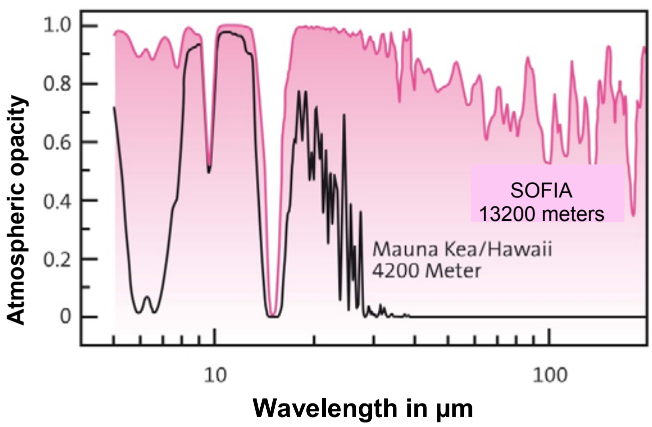

Transmittance of the atmosphere at Mauna Kea (Hawaii, black line) and in the stratosphere (pink line, altitude of SOFIA). The far-infrared (FIR, from 30 microns) is not observable from the ground. (Röser/SuW-Graphik).

Application in astronomy 1: Stars and the laws of radiation

Colors of the stars

In 1814, German optician from Munich, Joseph von Fraunhofer (see picture), examined the solar spectrum and made an important discovery: The spectrum of sunlight showed narrow dark lines. He determined the intensity of solar radiation at different wavelengths and found that the maximum of the energy radiated by the Sun lies in the yellow-green region (see below, the curve above the solar spectrum, drawn by Fraunhofer; it is called a ‘spectral energy distribution’ (*Astronomische Nachrichten*, 1874).

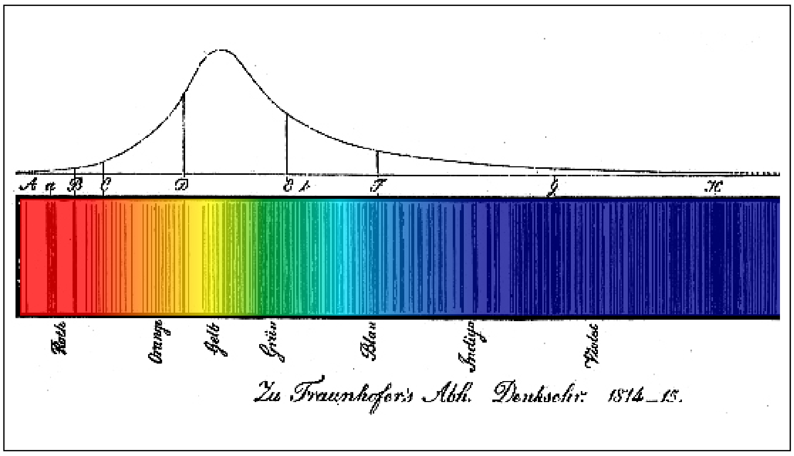

The Sun, however, does not appear to us yellowish-green; we see a yellowish-white sun. Why is that? The reason for this color perception is the combination of all colors of sunlight that takes place in our eyes.

A careful look at the stars in the night sky reveals that not all stars are yellowish-white. Some appear white, others shine blue and some others appear red. This is due to Wien's displacement law, according to which the maximum energy radiated by the stars varies as a function of their surface temperature and thus lies at different wavelengths. Their colors change accordingly.

Right image: The Orion constellation. Different colors of the stars can be clearly distinguished.

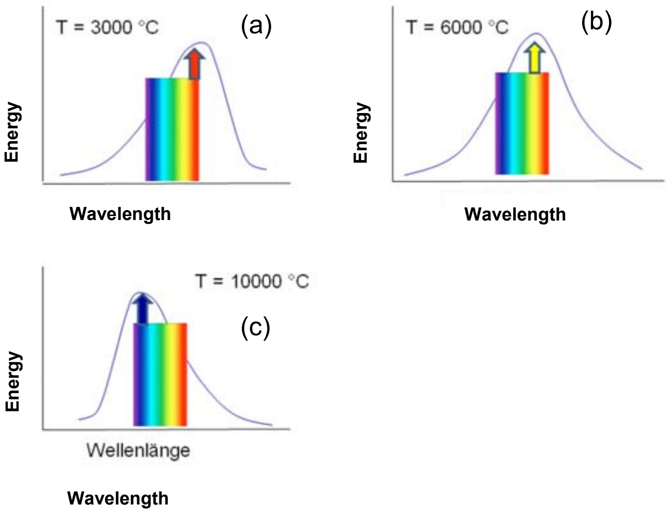

The Planck curves in the diagram indicate the spectral energy distributions of three different stars. As shown, cool stars (a) with T ~ 3000 °C (3273 K) emit most of their energy in the red area of the spectrum. They therefore appear reddish. The Sun, with a temperature of 6000 °C (5778 K), radiates energy most strongly in the yellow-green region (b). Hotter stars, however, radiate most of their energy in blue wavelengths and appear therefore blue (c).

Hence, there is a physical relationship between the surface temperature T of a star and its color. From astronomical observations we find that the surface temperatures of stars range between about 30,000 Kelvin (K) (blue stars) and 2000 K (red stars). Sun-like stars (yellow and yellowish-white stars) have surface temperatures of about 5000 to 7000 K.

Astronomers have assigned spectral types to stars based on certain spectral lines. Initially, the spectral types were ordered alphabetically. Later, the order was changed according to the observed surface temperatures. Therefore, the current order of the essential spectral types of stars is: O, B, A, F, G, K and M. The table below shows the approximate ranges of temperature and colors that correspond to the respective types of stars (spectral types).

Surface temperature (K)	**Color of star**	**Spectral type**	**Example (bright star)**
30000 – 60000	blus	**O**	Mintaka (δ Orionis)
10000 – 30000	blue-white	**B**	Spica
7500 – 10000	white	**A**	Sirius
6000 – 7500	yellow-white	**F**	Procyon
5000 – 6000	yellow	**G**	Sun
3500 – 5000	yellow-orange	**K**	Arcturus
< 3500	red	**M**	Beteigeuse

The sequence of spectral types within this classification can be accomplished with an easy to remember mnemonic:

‘**O**h **B**e **A** **F**ine **G**irl, **K**iss **M**e’ or ‘**O**h **B**e **A** **F**ine **G**uy, **K**iss **M**e’

Maybe you can invent a better one?

Stars form in clouds of gas and dust that are present in the disk of the Milky Way. They come with different temperatures and colors according to their masses and stages of development. Depending on their initial mass, they undergo different stages of development at different rates and their final stages differ accordingly. The figure below indicates the evolution of stars of four different initial masses.

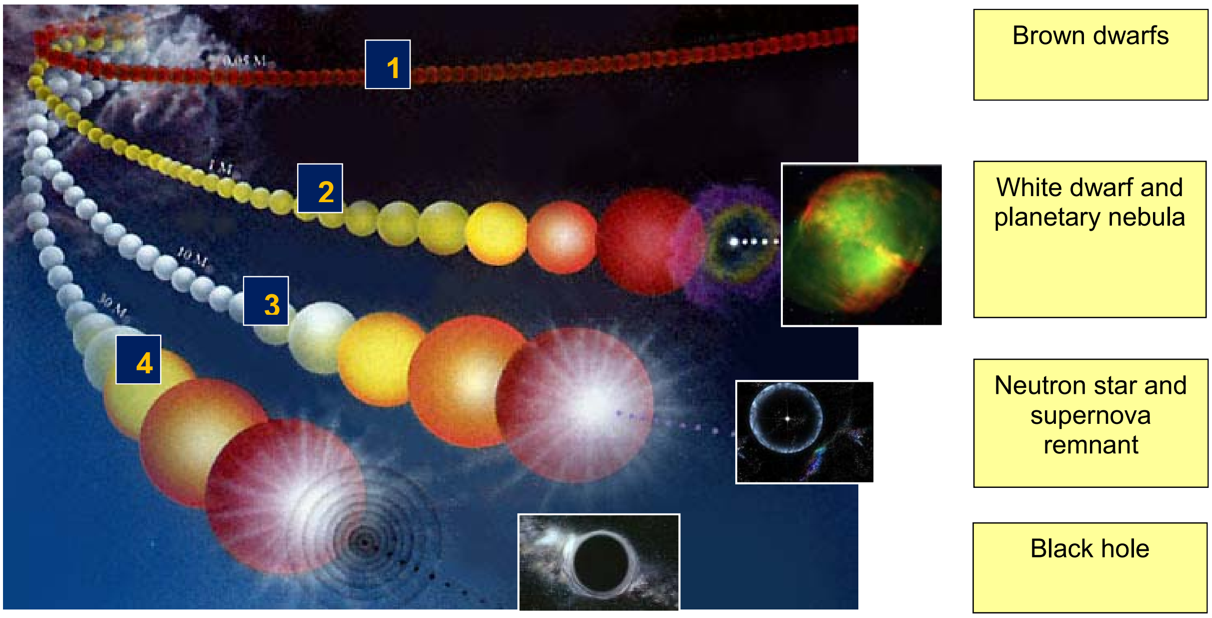

1. **Brown dwarfs** are created when the mass of the protostar is less than about 0.08 solar masses (the mass unit for stars is one solar mass: 1 $M_\odot$). This mass is not sufficient to ignite fusion of hydrogen into helium in the center. Therefore, a brown dwarf actually is not a star, but rather an object between star and gas giant planet. Depending on mass and age, the surface temperature of a brown dwarf lies in the range of about 600 - 3000 K (corresponding to the new spectral types L and T). Thus, brown dwarfs primarily radiate almost entirely in the infrared (Wien's law).

2. **Solar-type stars** shine yellow like the Sun. They reach an age of about 10 billion years. When their nuclear energy is exhausted, they expand and become a red giant. Finally, they lose their outer layers (resulting in a planetary nebula) and the core becomes a white dwarf (about Earth-size).

3. **Stars with masses greater than about 10 $M_\odot$** develop faster, because their consumption of nuclear energy occurs faster (lifetime about 15 million years). They end up as red supergiants and terminate their lives by a huge explosion, a supernova. The remaining core shrinks and becomes a very dense object, a neutron star.

4. **Stars with masses greater than about 30 $M_\odot$** have a fate similar to stars of 10 $M_\odot$, but they live even shorter. When one of these stars finally explodes as a supernova, the core collapses so completely that it becomes a black hole.

Activity 2: The ‘Spectrino’ - A model for visualizing the electromagnetic spectrum

The ‘spectrino’ is a model that illustrates the band of spectral regions using a linear axis for the wavelength. It visualizes spectral colors and indicates that there is radiation other than visible light. You will need the hand spectroscope and your mobile phone camera or other digital camera.

Activity 2.a

Turn the Spectrino on. You can see the appropriate colored light-emitting diodes (LEDs) UNDER the color strip, which indicates the visible part of the spectrum. Look through the spectroscope at the light of the LEDs and compare that with the continuous spectrum of a light bulb. Describe your observations.

Activity 2.b

What about the LEDs on the right side of the Spectrino? Are they broken? Take your cell phone camera and look at them. Describe what you see. How can you verify the components of radiation that are invisible?

Activity 2.c

The infrared range (NIR, MIR, and FIR together) of the electromagnetic spectrum in a linear wavelength scale is larger by a factor of 944 than the visible range range (380-750 nanometers (nm)). How big is the IR range on the scale of the Spectrino model?

Activity 2.d

As an addition to the linear wavelength scale, mark the visible and infrared areas in the decimal logarithmic scale given below. How did you determine the range borders?

10^2 nm **10^3** **10^4** **10^5** **10^6**

3. The near-infrared (NIR) – Detection and properties

Activity 3: The remote control: A NIR radiator in your living room

Remote controls are common objects to us. Many people, however, are not aware that the remotes emit infrared radiation.

Activity 3.a

Take a remote control and press on one of the keys, while a classmate observes the remote's infrared LED with his or her mobile phone camera. Change places with your classmate. Describe your observations.

Activity 3.b

Look for possibilities to divert the signal of the remote control 'around the corner'. Describe and explain your ideas.

Physics Information Box

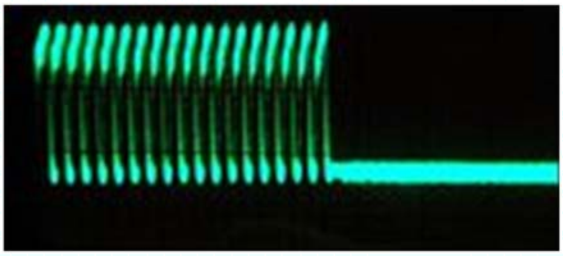

38 kHz-carrier signal, ©Ebuss (wsrp)

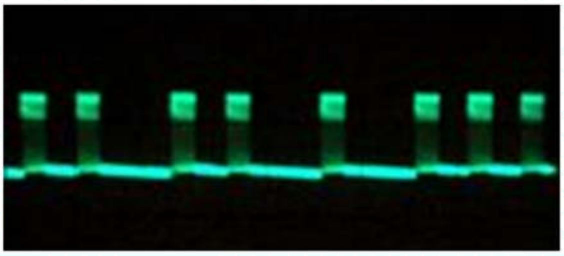

Modulation of the 38 kHz-carrier signal into a special bit sequence, ©Ebuss (wsrp)

Infrared remote controls send out IR signals with, for example, a 38 kHz carrier frequency (top left). This otherwise rarely-occurring frequency allows for transmission without interference. The carrier of the signal is modulated with a sequence of pulses; 21 wave trains of the carrier signal result in one pulse (picture on top left indicates the largest part of a pulse). The pulse has a duration of about 0.5 ms.

The pause length between two pulses allows for binary coding: A pulse with the same following pause corresponds to bit 1, a pause twice as long corresponds to bit 0. Each time you press a button on the remote control, a precise bit sequence is generated. The sequence is sent out repeatedly, as long as you push.

Activity 3.c

The sequence of pulses (right image in the info box) from the remote control has a certain (average) frequency, which you should determine by counting the pulses in the image. The duration of the breaks in between is either as long as the pulses or twice as long. Because of the varying pause length, we consider the average frequency.

Activity 4: Making NIR radiation audible

(Dana Backman, SETI Institute)

Although light waves and sound waves differ in many respects, their wave character is common. Accordingly, we will make some comparisons.

Activity 4.a:

Find out about the frequency ranges of seeing and hearing, and compare them. What did you discover? What is an octave? How many octaves are included in the hearing frequency range? How large is the frequency range of visible light compared with music intervals? Of IR light?

Activity 4.b:

Examine the NIR light sent by a remote control using a solar cell, which is connected with a speaker that translates the light pulses into audible sound frequencies. Compare the pitch with the frequency in activity 3.c.

Activity 4.c:

Between which colors is there 'harmony' and 'discord,' so to speak? (see information box on Music)?

Physics Information Box

Electromagnetic waves with wavelengths from 380 nm to 750 nm (that corresponds to frequencies from 400 to 789 Terahertz (THz)) appear to us as visible light. The infrared and ultraviolet ranges are outside this wavelength range and are invisible for us.

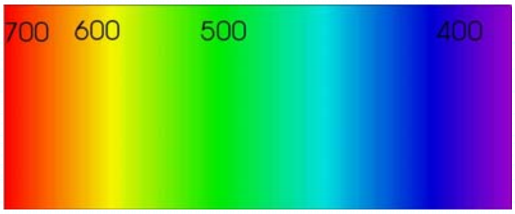

The respective spectral color areas (color perception of light with different wavelengths) are as follows:

Red: 630-750 nm, Orange: 590-630 nm, Yellow: 570-590 nm, Green: 495-570 nm, Blue: 435-495 nm, Violet: 380 nm-435 nm.

Audible sound waves have frequencies between 16 Hz and 20 kHz, far below the frequencies of light. A light signal can be pulsed with audio frequency (converted to a pulsating current flow by means of a solar cell) and thus can be made audible with an active speaker (speaker + amplifier).

Music Information Box

An arbitrary note in music together with the keynote (tonic, or fundamental tone) forms a musical interval that is characterized by a certain frequency ratio (f_{note} / $f_{keynote}$). The intervals are as follows:
Unison (1:1), major second (9:8), major third (5:4), perfect fourth (4:3), perfect fifth (3:2), major sixth (5:3), major seventh (15:8) and octave (2:1). Perfect fourth and perfect fifth are harmonies,, major second and major seventh are discords (dissonances) to our ears.

Activity 5: Light emission processes and the energy-level diagram

(for senior classes)

Use the provided NIR indicator card to detect the NIR radiation of a remote control or any other source.

5.a:

Determine the wavelength of the light emitted by the card by means of its color (a hand-spectroscope with wavelength scale will be helpful). Examine the dependence of the detecting capability of the card as a function of the duration of exposure of NIR light. The experiment should be carried out in a very dark room. Carefully describe the results of the experiments.

5.b:

A luminescent material emits green light (λ = 550 nm) after exposure to infrared radiation. Calculate the wavelength of the IR radiation in case of two-photon absorption (see the Physics Information Box below, case IV).

Physics Information Box

The **energy level diagram** illustrates the quantized (discrete) energy transitions of electrons in the atomic shells. These transitions can be accompanied by absorption or emission of photons, but can also take place without any radiation.

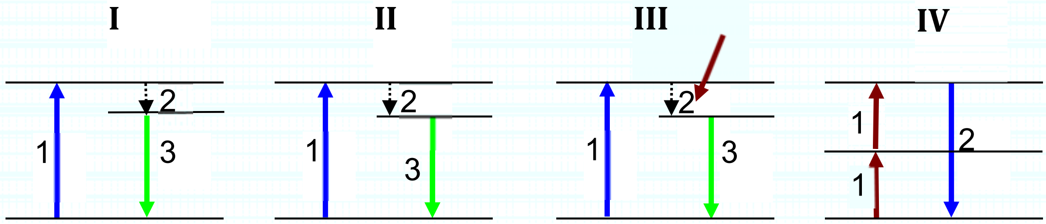

Case I - Fluorescence: The electron is excited from the ground level to a higher energy level due to absorption of a light quantum (e.g. UV) or due to collision (1). There, it loses more or less of its energy – depending on the fluorophore crystal - without radiating and normally, without delay, thus moving to an intermediate energy state (2). Then, it radiates away the remaining energy as a lower-energy photon (3).

Case II - Spontaneous phosphorescence: Steps (1) and (2) are similar to case I, except for the fact that in the phosphorescing crystal, the electron stays for a longer time in the intermediate state than in case I. The remaining energy is emitted spontaneously, but with a time lag, as a lower-energy photon, i.e. the crystal remains illuminated for some time after the excitement (3).

Case III - Phosphorescence after IR stimulation: Steps (1) and (2) again are same as in case I. This time, however, the spontaneous emission from the intermediate state occurs only rarely. The remaining energy is stored until an IR photon stimulates de-excitation (3).

Case IV - Fluorescence after two-photon absorption: Certain phosphors allow the absorption of a photon (e.g., IR photon) and quasi-simultaneously the absorption of another photon while in the temporary intermediate state (e.g. again IR, (1)). An excited state is reached with the sum of the absorbed energies, which de-excites by emitting a visible photon (2).

Activity 6: Properties of NIR radiation – Reflection

The NIR transmission image of a surveillance camera or a webcam can be displayed on a computer screen. You will need an adapter to connect the video output of the camera to the USB port of your computer. Look at, compare, and describe the images of different test objects in visible light and in near infrared.
Examine:
a) Plant leaves on a green background,
b) A 20-dollar bill,
c) A bare arm.
You should perform this experiment in a darkened room. Try to give an initial explanation of your observations.

Questions: How do the leaves appear in the NIR? Describe your observations of the dollar bill and the bare arm. Why do the pupils of the eyes appear white, when observed with NIR light? How does a NIR surveillance camera work?

Physics/Biology Information Box
The wavelength dependence of reflection, transmission, and absorption determines the colors of our environment. Photographic IR, images allow new views. Chlorophyll (green of leaves) appears brilliant white at NIR wavelengths (below 'Wood effect'), because chlorophyll is transparent at infrared wavelengths, and because the cell structure of the leaves reflects very strongly in broad NIR bands.

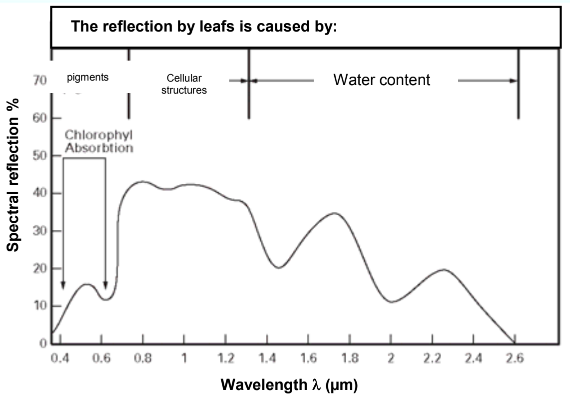

Geography Information Box – Remote Sensing of the Earth
The difference between reflection in visible light and in NIR can be used for detection of photosynthesis and of the growth of plants. Thus, the Wood effect is important for the **Remote Sensing of Earth**, regarding biological and ecological aspects (preparation of vegetation maps). The image shows vegetation maps of Europe and Africa in January and in July. Green color indicates strong growth, brown color stands for the lack of growth (Image: eduspace.esa.int).

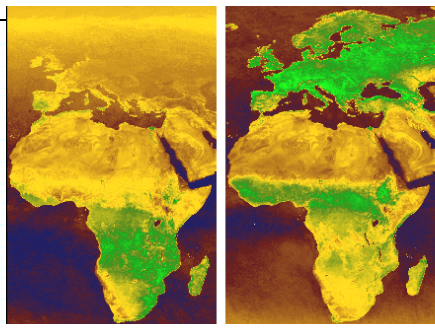

Activity 7: Properties of NIR radiation – Transmission and Absorption

Prominent differences between visible and NIR light also exist in terms of transmission and absorption. In this experiment, we will examine Coke. We look at a test object in visual and in NIR light through Coke, i.e. after transmission of the light through Coke. To visualize the NIR image, again, we use a surveillance camera or a webcam plus NIR illumination. The experiment should be performed in a very dark room.
Describe your observations and try to find an explanation.

Physics Information Box

The ratio between the radiation intensity that exits a medium (I_1) and the radiation intensity that initially enters into the medium (I_0), i.e. the fraction of transmitted light, is called *transmittance T*. The non-transmitted portion of the medium is called *absorbtion* (or absorption coefficient) *A*.

$$T = \frac{I_1}{I_0}, \qquad A = 1 - T = 1 - \frac{I_1}{I_0}.$$

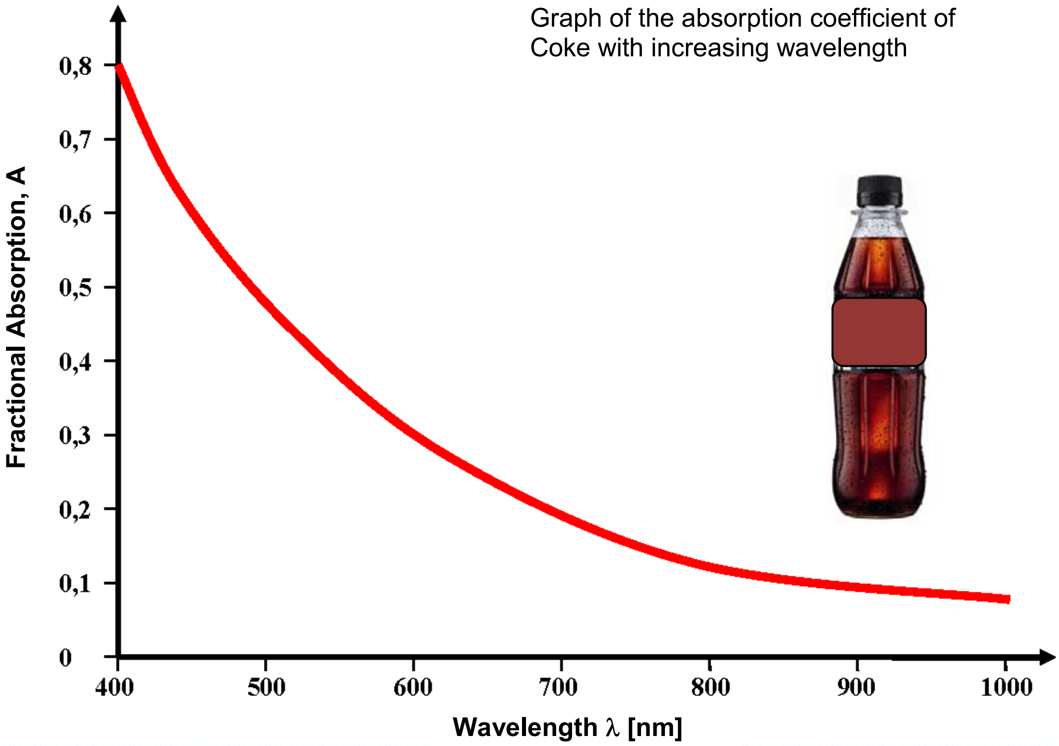

Calculation exercise: Suppose 10^6 visual photons (with $\lambda \approx 500$ nm) and just as many NIR photons ($\lambda \approx 920$ nm) are directed into the Coke. How many photons of each wavelength can pass through?

Application in Astronomy 2: Seeing the Galaxy through dust clouds

Between wavelengths of 0.8 and 1.1 microns, the same astronomical observational methods are applied as for visible light. Hot blue stars, which are prominent at visible wavelengths because of their high temperatures, 'fade' away in the NIR. Cooler stars (red giants and red dwarfs) are relatively prominent in at NIR wavelengths.

Visible (left) and NIR image of the Galactic Center. Visible Image: ©Howard McCallon Infrared Image: ©2 Micron All Sky Survey (2MASS)

The left picture above, made at visual wavelengths, shows three groups of stars in the dust belt (bluish in the middle, reddish at bottom right), whereas in the NIR image on the right, those stars are almost not recognizable. The NIR image, in turn, shows cooler reddish stars that are less apparent at visible wavelengths. These stars are mostly red giants.

Seeing through dust

Interstellar dust, found in the gas and dust clouds of the Milky Way's disk becomes more and more transparent (translucent) with increasing wavelength because dust absorbs NIR less than visible light. This is due to the fact that the wavelengths of NIR radiation are larger than the average diameter of dust particles. Dust particles efficiently absorb radiation with shorter wavelengths than their diameters. Thus, NIR observations allow a view deeper into the birthplaces of stars, as the images of the dark cloud Barnard 68 (B68) clearly show (right image in NIR, left image in visible light, images: ESO / VLT).

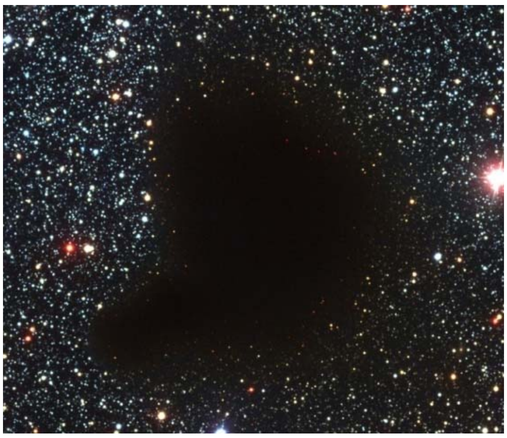

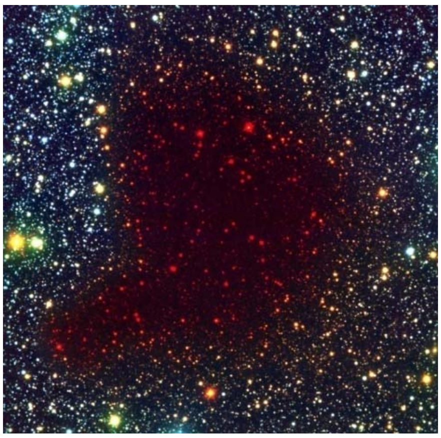

Activity 8: The dark nebula model

The so-called dark nebula model demonstrates how astronomers are able to discover stars in or behind cosmic dust clouds. Stars are represented by NIR-emitting diodes, which are installed within a wooden panel, which in turn is placed behind a photo of dark nebula. Thus, a light source that is actually invisible to the eye can be detected by a digital camera.

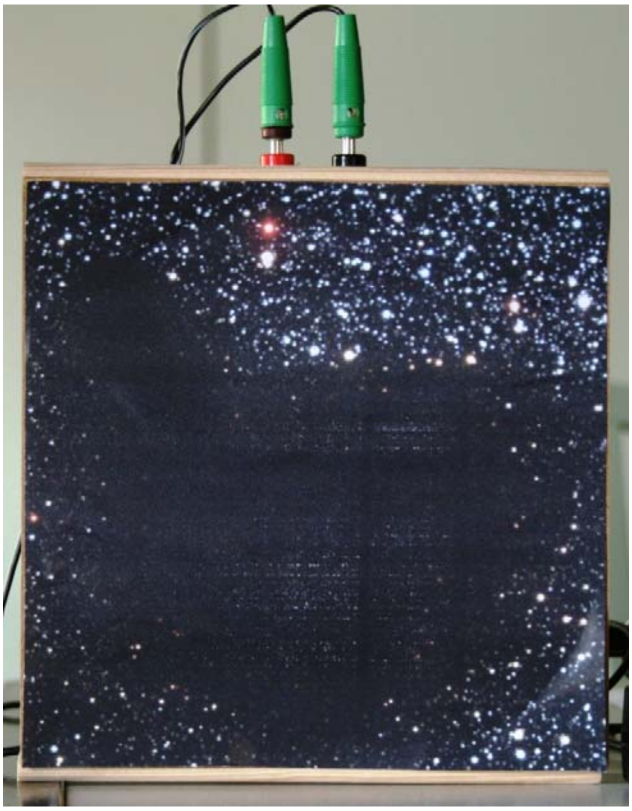

Since the model can be constructed easily and without much effort, it qualifies for an introduction to IR astronomy. When building this model, the students put their knowledge of electric circuits into practice. This serves as an important and positive experience. The model allows a simulation of astronomical work: the coordinates of stars can be determined with the help of the observed model stars on the photo.

Activity 8.a: Constructing the dark nebula model

Instructions

1.) Cut out the photo of nebula B68 (18 cm x 18 cm) and cut the MDF plate accordingly.
2.) Mark the positions of the five model stars on the board, according to their respective positions in the dark nebula photo. (You can use the positions of the stars on the NIR photo of B68.)
3.) Drill five holes for the LEDs (5 mm drill bit) and extend the holes from the back side with a 6 mm drill bit with a depth of 3 mm.
4.) Now think about how to switch the 5 LEDs together, so that the current flows in the correct direction without exceeding the circuit capacity (!). If the voltage of the AC adapter suffices, you may, for example, connect the 5 diodes in series and find the exact adjustment by a series resistor. (A series resistor is necessary anyway to limit the current.) A combination of series and parallel connection offers a range of opportunities. You should sketch the course of the circuit with a pencil and clearly mark the polarity.
5.) Now you can plug in the 5 LEDs from the rear side (pay attention to the polarity: the flat side of the diode marks the cathode, i.e. the negative pole).
6.) In order to connect the diodes, the connection wires mostly suffice. You should bend the wires according to the circuit diagram. In each case, two adjacent connecting wires end on the top of a thumbtack, which previously was pressed into the board. There, you should solder them together. (The thumbtacks simultaneously connect the circuit with the board.)
7.) Complete the circuit by installation of the series resistor so as to limit the current in the connecting wires that lead to the jacks of the banana plugs (or just to a insulating screw joint). There, the AC adapter is connected in the end: mark the polarity. You can also install a push-button switch.
8.) Attach the banana plugs with the power supply in the power adapter.

Fixing the positions of the LEDs.

Pressing the thumbtacks.

Soldering the LEDs.

9.) Now, saw off two 18 cm and two 19 cm pieces from the 5 mm thick and 4 cm wide wooden border. Make a frame for the plate out of the borders with glue and nails, so that the edges rise about 5 mm above the image plane from all sides. On the back side, the 25 mm excess length protects the circuit and allows the model to stand vertically. Build in the current sockets for power supply into the border and possibly also a push-button switch.

Placing the frame.

10.) Place the photo into the frame; cover it with an inconspicuous transparent film.

11.) A functioning test with a digital camera will show whether the connections are conducting. If the LEDs do not work, you can gradually check the circuit using a simple universal test meter.

Material list

- An empty yogurt cup with:
  - Five NIR-emitting diodes (5 mm) of the type: TSAL 6100 (940 nm) or TSHF 5410 (890 nm) or LI521 (870 nm), or ...
  - Two sockets (4 mm, 10 A) and 2 banana plugs; alternatively: 1 terminal block, including a small 10 mm wood screw
  - One push-button switch
  - Ten thumbtacks (brass plated steel)
  - 20 cm of wire
  - Resistors as needed (depending on the output voltage of the AC adapter)
- Wall Power Supply e.g. 9 V DC, 250 mA (power source possibly from physics collection)
- Medium-dense fiber board (MDF plate, 18 cm x 18 cm x 1 cm)
- Wooden border (80 cm x 4 cm x 0.5 cm)
- Ten nails (about 2 cm length)
- Possibly 2 small screws for wood (10 mm length)
- Glue for wood
- Two square color prints of identical size and location of images of the dark nebula Barnard 68 (B68) or the cone nebula (or ...) in the NIR and in visual light, size 18 cm x 18 cm
- One transparent film as a protective cover for the photo

Tools list

- Electric drill
- Drills for wood (5, 6, 8, 10, 12 mm)
- Small locksmith’s hammer
- Side cutters, wire strippers, possibly gripping pliers
- Coping saw, sandpaper
- Scissors, knife, cutter
- Soldering equipment (soldering iron, deposit, tin-solder, possibly flux)
- Screwdriver for terminal block
- Phillips screwdriver for small wood screws
- Multimeter, 2 connecting leads, 2 alligator clips
- Ruler, triangle, pencil, eraser

The complete model (an older version that is bigger and not square) is now ready for testing.

Activity 8.b: Coordinate determination with the dark nebula model

Take a shot of the B68 dark nebula model using your digital camera with NIR diodes switched on. The photo shows some stars in the dark nebula area which are not visible with the naked eye. Print out the picture or show it with the computer monitor. Take stars 1 and 2 in the right figure as reference stars and determine the celestial coordinates (right ascension α, declination δ) of the 'newly discovered' star.

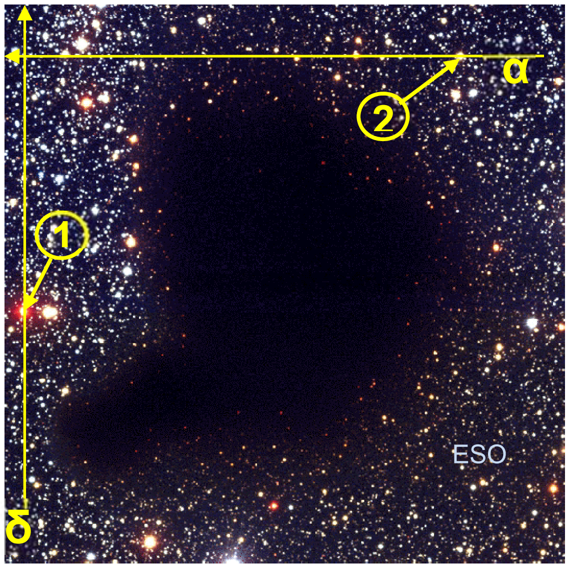

Star 1: $\alpha = 17^h\, 23^{min}\, 23^s$, $\delta = -23°\, 50'\, 43''$

Star 2: $\alpha = 17^h\, 23^{min}\, 6^s$, $\delta = -23°\, 48'\, 31''$

Assume a Cartesian coordinate system for the description of the coordinates in this section of the sky; the axes (α-axis and δ-axis) of the Cartesian system run as shown in the figure.

Procedure

Measure the distances in the α- and δ-directions on the photo with a ruler or on the screen with the mouse (pixel ratio). Convert the distances specified in millimeters or pixels into time measure (for α) and degrees (for δ). The reference stars serve as scale. You get the final coordinates by simply adding or subtracting the results from the coordinates of the reference stars 1 and 2 (*1 and 2 are the reference stars).

Star #	Distance to reference star 1 in α-direction (mm or pixels)	Distance to reference star 2 in δ-direction (mm or pixels)	α (h min s)	δ (° ' ")
1*	0		17h 23min 23s	-23° 50' 43"
2*		0	17h 23min 6s	-23° 48' 31"
3				
4				
5				
6				
7				

Mathematics Information Box

In astronomy, different spherical coordinate systems are used. The equatorial coordinate system (fixed relative to the apparent celestial sphere) is described by the declination δ (corresponding to the latitude of the Earth) and the right ascension α (corresponding to the longitude on Earth). While δ is measured in degrees (°), arc minutes (') and arc seconds ("), the time units hours, minutes and seconds (h, min, s) are used for α.

The rotating Earth means: 360 ° → 24 h (Fig. GNU-FDL).

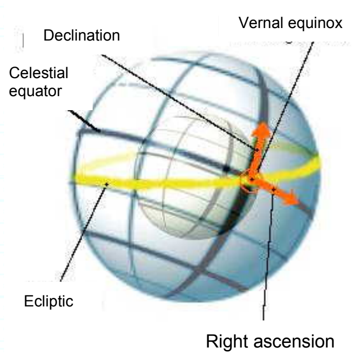

Application in Astronomy 3: The mass of black holes

Astronomers have evidence that a supermassive black hole exists in the center of the Milky Way. Dust clouds in the plane of the Milky Way impede the view to the Galactic Center (left image). Only NIR observations made it possible to see into the central regions of the Milky Way (right image).

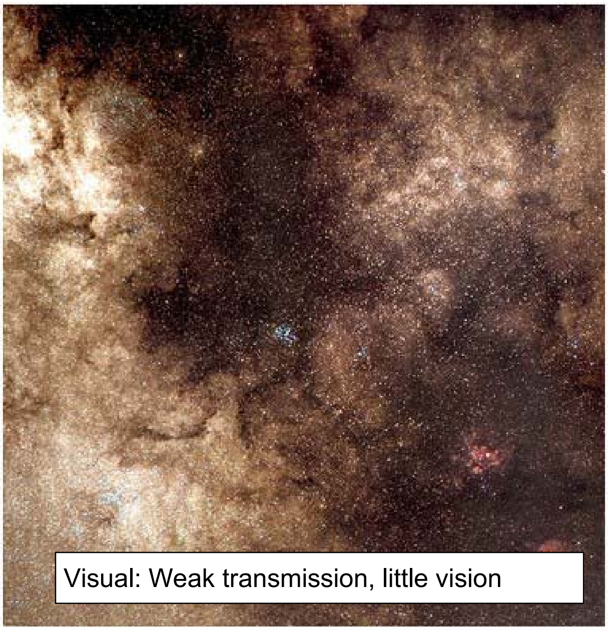
Visual: Weak transmission, little vision

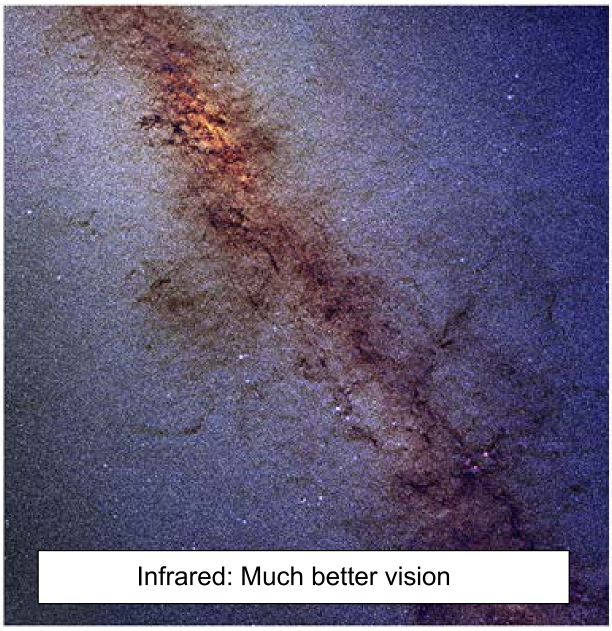
Infrared: Much better vision

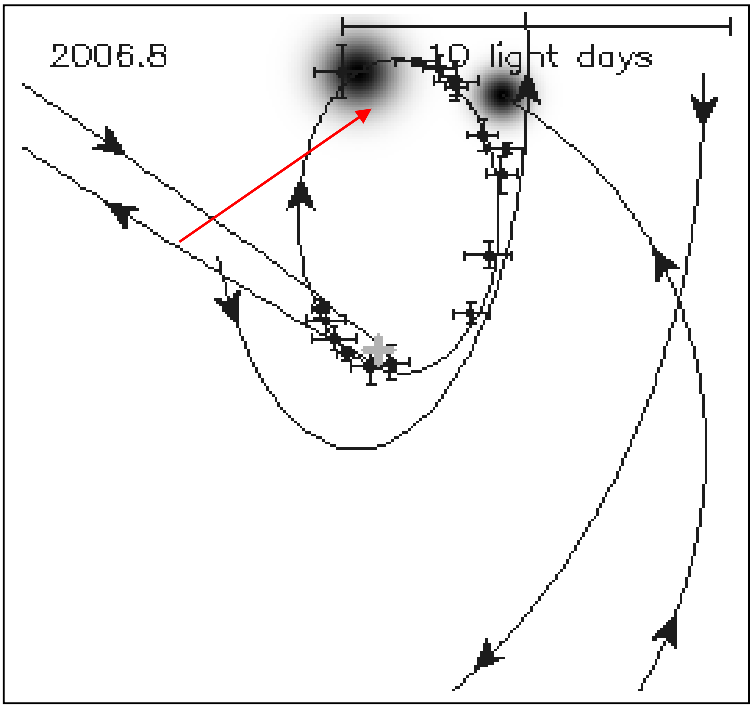

NIR wavelengths allow the observation of stars that are located near the center of the Milky Way. Observations of the positions of these stars over many years enabled the determination of their orbits (the orbits of five stars near the center are shown in the diagram). From these observation a central mass of about 3.7 million solar masses could be determined by means of Kepler's third law. Of that total, 2.6×10^6 (2.6 million) solar masses are in the supermassive black hole (arrow). Useful material can be found on the webpage www.wissenschaft-schulen.de.

4. The mid-infrared (MIR)

The MIR region of the electromagnetic radiation ranges from 5 to 30 micrometers (microns) wavelength. Below, you can acquire or refresh some physical background. After a brief introduction into how a MIR camera works, you can use the camera and thereby make amazing discoveries in the world of the mid-infrared.

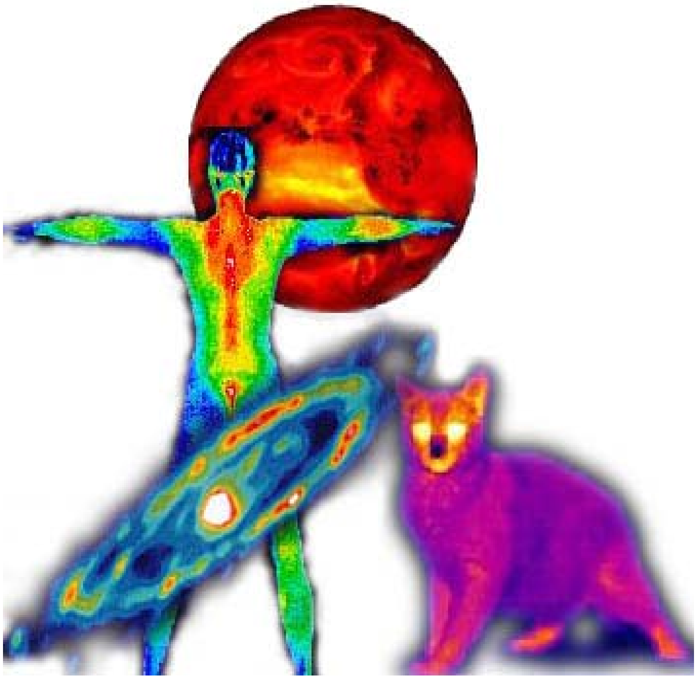

According to Wien's displacement law, bodies with emission maximum in the above-mentioned wavelength range have temperatures of about 150 - 600 K. Thus, bodies at room temperature (about 20 °C or 293 K) emit in MIR with maximum intensity at a wavelength of about 10 microns. Thus, in order to view our environment a camera should be used that is sensitive to wavelengths in the MIR range of about 10 microns. Commercial MIR cameras operate at about 8 to 14 microns.

The total radiation output of a body rises according to the Stefan-Boltzmann law (see above, section 2.2) strongly with temperature. *This relationship is used to quantify the temperature of a body from the received intensity of radiation*. Therefore, MIR cameras are also called thermographic cameras.
However, not all the radiation that we receive from a body is also emitted from this body. In addition to its emission, reflection and transmission of radiation of the environment have to be considered.

The world of the mid-infrared is very different from the world of visible light. While the light that we see with our eyes comes mostly from reflected radiation of the visualized objects that ultimately comes from the Sun or artificial light sources, the radiation in the MIR is determined primarily by the emission of the objects viewed. Transmission also shows differences. Air is transparent (transmissive) only in certain MIR spectral ranges. Water and glass are not transmissive for MIR; they absorb in this range strongly. Also, the reflection properties of MIR are different from those of visible light; the scale of surface roughness generally determines the respective reflection type (specular or diffuse).

4.1 How do thermal IR cameras work?

The two basic functions of thermal IR (thermographic) cameras are the quantitative measurement of an object's temperature and the visualization of MIR radiation in a thermal image. Thermal images are false-color images displaying MIR information.

There are different types of cameras, distinguished by several criteria. The detected wavelength range is one classification criterion. 'Shortwave' cameras (sensitive to 2 - 5 microns, actually in the astronomical NIR) are distinguished from 'Long Wave' cameras (sensitive at 8 - 14 microns). Another criterion is the different imaging principles.

Focal Plane Array cameras (FPA) cameras are widely used. The optics of this type of camera is basically the same as an ordinary digital camera: a lens transfers the radiation onto a detector array. But, a MIR-transmissive lens is made, for example, of germanium rather than glass, Also, a MIR detector array is not the same as a CCD: a separate self-contained MIR detector exists for each pixel.

We also distinguish between cooled and uncooled systems. Uncooled FPA cameras are cheap to use. Their detectors are called bolometers, consisting of a semiconducting material (eg, vanadium oxide) that changes its resistance corresponding to its temperature caused by the absorbed incident radiation.

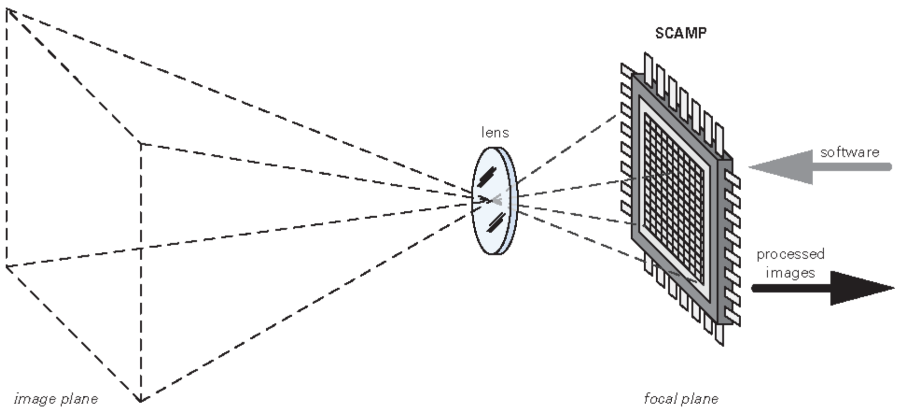

The thermal image is produced when each pixel's measured resistance is converted into a color value. Uncooled cameras have less sensitivity and accuracy. Therefore, FPA cameras are cheap (about 4000 euros) and also small & portable. However, the camera must often be calibrated. Moreover, the bolometers influence each other through thermal conduction.

Applications of thermal IR cameras

Thermal IR cameras are being used increasingly. They were originally developed for the military, and are used even today as night vision and target detection systems for missiles. Fire fighters use MIR cameras when working in the dark, especially in dense smoke and fog. Humans can be detected through their body radiation in the MIR well and thus can be saved. In medicine, MIR cameras allow a rapid diagnosis, for example in the detection of vascular diseases (see picture below).

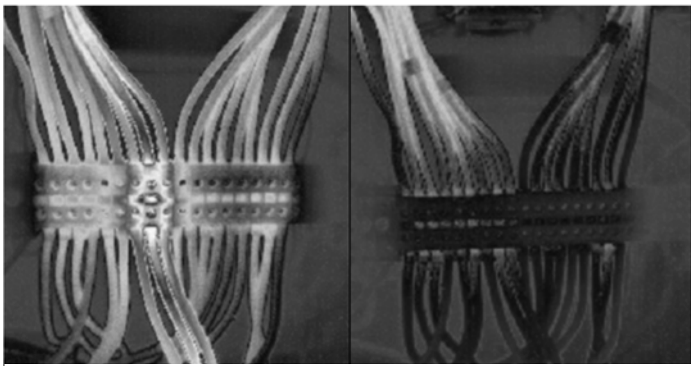
Application of thermography: Defective (left) and functioning wire connection.

In civil engineering, there are several applications for thermography. Leaks in pipes can be made visible. For this task, hot gas is pumped into the leaking pipe, heating the location of the leakage. This heat is then detected by the camera. Also, the insulation of buildings can be checked through this method. Heat escapes much quicker from poorly insulated points. Heating pipes in floors can be tracked easily.

There are also many applications for MIR cameras in industry. During cooling, after the casting of metal or plastics, a uniform temperature distribution is necessary. This can be controlled by thermography. Electronic components or mechanical parts heat up when they are defective or overloaded. This can be detected quickly by a thermal camera. In the picture above, a defective cable connection and a functioning one are compared.

Many sciences also use MIR cameras. In geology, for example, certain rock structures and compositions can be detected. In astronomy, use of thermal IR cameras allows direct detection of interstellar dust that is not hot enough to radiate at visible wavelengths.

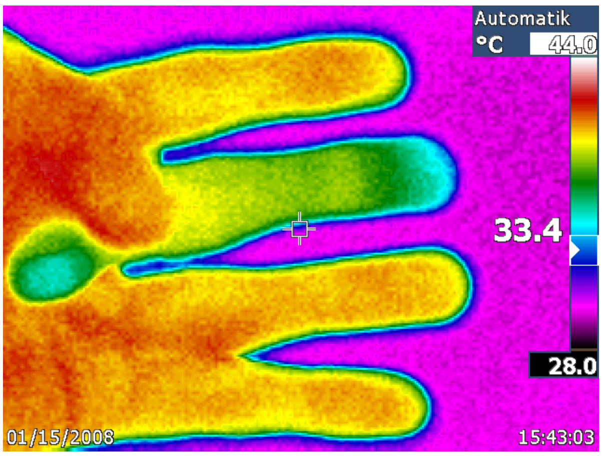

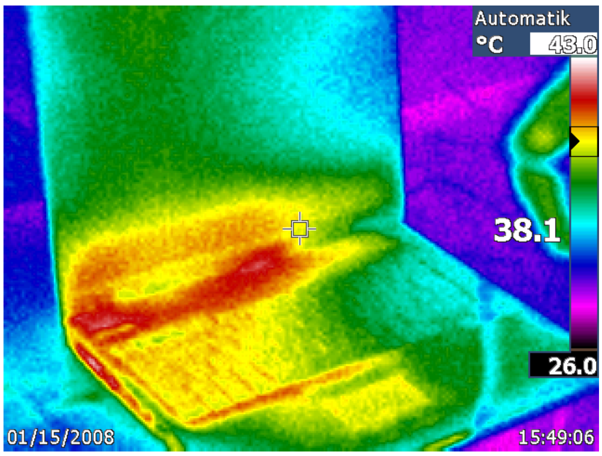

Activity 9: Emission of MIR radiation

(You will need a thermal IR camera for these experiments!)

Examine various objects, including your body, with a thermal IR camera. Write up the results into a table and compare the images in the visual with the MIR.

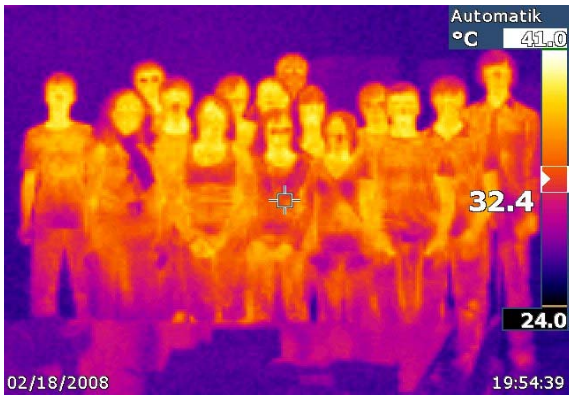

Persons in visual light (left) and in MIR (right).

Activity 9.a:

Observe by means of the thermal IR camera people with and without glasses. What do you find, and why?

Activity 9.b:

Some of you rub your hands together vigorously for about 10 seconds and then press them firmly for five seconds on a table. Observe that spot with the thermal IR camera immediately after removing the hands from the table. What do you find here, and why?

Activity 9.c:

Take a chilled beverage bottle and press it for ten seconds on your cheek. Scan your face thereafter (without the bottle) using the thermal IR camera. Describe your observations and try to find an explanation.

Activity 9.d:

Hold a black garbage bag in front of the face of a classmate and take a photograph with the thermal IR camera. Repeat the experiment with a blown up balloon. Write down your observations and try to find an explanation.

Activity 10: Barriers to the infrared – Absorption in Earth's atmosphere

Activity 10.a:

Look at an IR lamp with a thermal IR camera through a transparent container half-filled with water. Look through it first through the water-filled part and then through the air-filled part.
Afterwards, use your hand to detect the IR part of the lamp radiation. Keep your hands first behind the water-filled and then behind the air-filled part of the basin (Image: DLR). Describe your observations in a table.

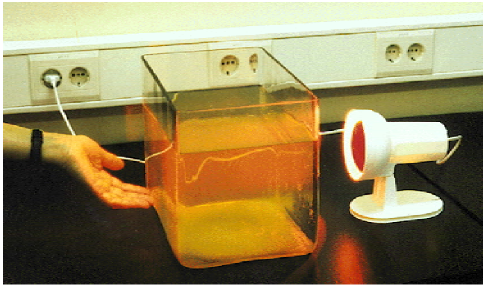

Activity 10.b:

Estimate the amount of radiation energy of the IR lamp that water ($c = 4.183\ \mathrm{kJ \cdot kg^{-1} \cdot K^{-1}}$) has absorbed, with measuring the temperature rise (e.g., within 5 min). What further information do you need? Try to find it. What assumptions have you made?

Activity 10.c:

Consider an analogy between the water molecule model in the IR kit and a mechanical damping element, used e.g. for seismic protection of buildings (see info box below). Arrange the size of the spring constant (large / medium / small) to the corresponding resilient connection.

Physics/Biology Information Box

Because of the v-shaped structure of the water molecule, there are three distinct normal modes of motion possible. Each of these modes absorbs the energy of incident radiation in a corresponding excitation frequency (resonance).

Absorption of NIR radiation occurs because of the symmetric stretch between the hydrogen atoms and the oxygen atom. Bending of the molecule is responsible for absorption in the MIR, and rotational transitions of the whole molecule for absorption in the FIR.

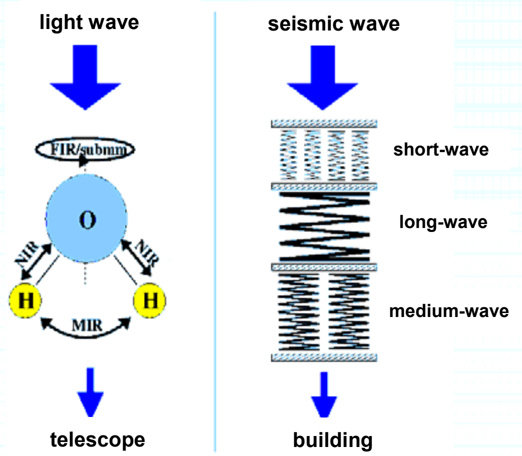

Application in astronomy 4: Radiation from cold objects

Observations in the NIR have been made from ground-based telescopes since the 1960s. Ground-based observations in the MIR are only possible from exceptional sites and over limited wavelength ranges. Observations in the FIR can only be made from locations above most of Earth's atmosphere because long-wavelength radiation is absorbed by atmospheric gases, especially water vapor and carbon dioxide (see diagram in section 3.3). That's why SOFIA carries a 15-ton telescope to altitudes of 13 km (43,000 ft) or more – above most of the IR-absorbing part of Earth's atmosphere. Note that, for MIR and FIR observations, the instruments must use very special detectors operating at temperatures near absolute zero.

Every object emits some thermal infrared radiation. According to Wien's displacement law, the wavelength of the strongest emission is inversely proportional to the emitting object's temperature.

Visual **NIR** **FIR**

(Images arranged by Robert Hurt, Caltech-JPL)

A celestial object appears quite different at different wavelengths. This is obvious in the pictures above of the Horsehead Nebula (also known as Barnard 33) in the constellation Orion. In comparison with the image taken in the visible range (left), the NIR image (center) shows many more (and cooler) stars. As mentioned already, interstellar dust is more transparent in the NIR, so stars hidden by dust can be detected. At even longer wavelengths, in the FIR (right), the emission of the dust itself is detectable. The warmer stars embedded in the cold dust are obscured by the strong long wavelength emission from the dust. Determination of dust density and distribution is important for understanding the evolution of stars, and is only possible via detection of FIR radiation.

In search of young planetary systems in the MIR

Young stars and planets evolve within protoplanetary disks. These disks consist of dense rotating systems of gas and dust that are normally found in or near huge molecular clouds located along the spiral arms of the Milky Way. As a protostar collapses, it warms up via release of potential energy and is detectable in the MIR range in contrast to the cooler background of the molecular clouds. Images of the Great Nebula in Orion (below) were taken at visual and NIR wavelengths. They show one of the most active star forming regions of the Milky Way. In this nebula many protoplanetary disks have evolved; you can see four of them in the middle image, with their respective central protostars appearing as light dots. Presumably, planets are forming in the outer regions of these disks. The image on the right shows a young star embedded in a protoplanetary disk viewed edge-on.

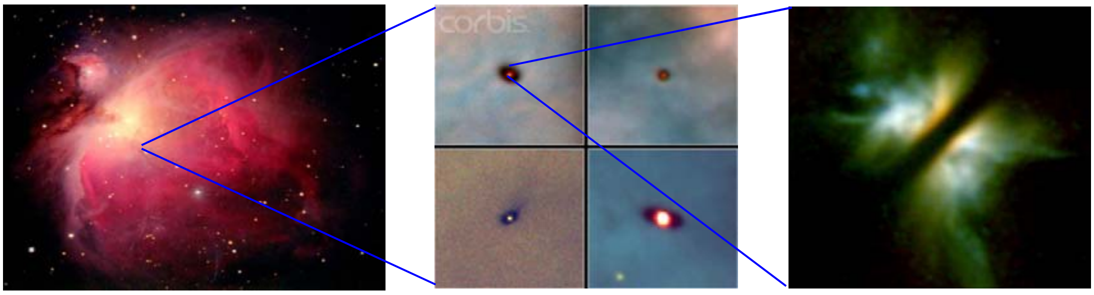

The process of forming a planetary system from dust particles takes millions of years. Dust particles in the micron range gather together to form planetesimals that are typically kilometers in diameter (like asteroids or nuclei of comets). This means that our solar system and other planetary systems initially consisted of 'oceans' of asteroids and comet nuclei. Planets form via planetesimal collisions and other processes. The figure below shows the different evolutionary phases.

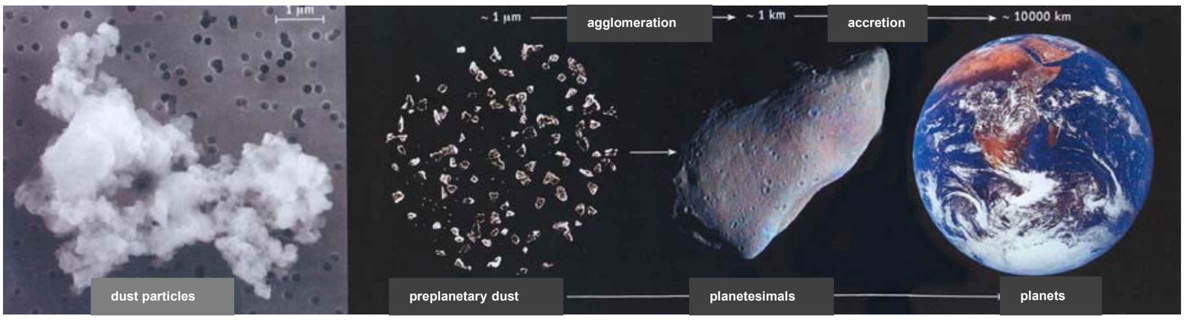

From dust to planets: dust particles accrete to become planetesimals (asteroids and comets) that collide to form planets. (Image from SuW)

Why are there Terrestrial and Jovian (gas giant) planets in the solar system? The underlying cause is understood to be the distance from the Sun at which a planet forms. Mercury, Venus, Earth, and Mars could gravitationally bind little or none of the gas from the protoplanetary disk because their proximity to the Sun subjected them to high temperatures and strong solar winds. The Jovian giant gas planets, forming far from the Sun at lower temperatures, could bind more gas around large rock cores and grow much more massive than the Terrestrial planets.

Cold object in our solar system detected in the MIR

Planets are not self-luminous at visible wavelengths – they are seen by reflected sunlight. The unreflected portion of sunlight is absorbed and heats up the planetary surface. The planet emits this heat as infrared radiation. The amount of heat emitted is dependent on the composition, structure, and temperature of the planetary surface.

Planets, moons, asteroids, and comets have temperatures from 50 up to many hundreds Kelvin and therefore mostly emit in the MIR. The atmosphere of Venus consists of 98% carbon dioxide, a 'greenhouse gas' that hinders the escape of MIR radiation. As a result, the temperature on Venus is almost 500 °C!

The visual-wavelength photograph at right shows a region of Phobos, one of Mars's two moons, near the 10 km-diameter crater Stickney. A spectral image taken with an MIR spectrophotometer allows determination of Phobos surface temperatures. The temperature in the shade is only 161 K, versus 268 K in areas exposed to the Sun.

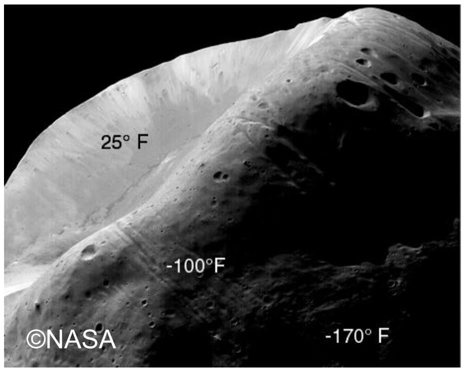

Do the math:
How to convert degrees Fahrenheit into Kelvin:
°F→K: $T_K = (T_{°F} + 459.7) \cdot 5/9$
How to convert degrees Celsius into degrees Fahrenheit:
°C →°F: $T_{°F} = T_{°C} \times 1.8 + 32$

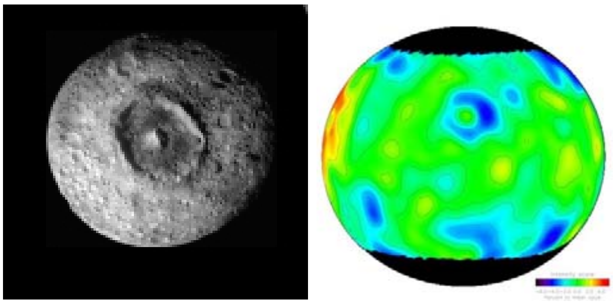

Asteroid Ceres at visual wavelengths (left) and in the MIR (right, false-color image).

Because the emission from asteroids is most intense in the MIR, observations in this spectral range are well suited to hunt for them. Infrared observations of asteroids can also be used to determine their dimensions.

The dust in comet tails emits MIR strongly as well. The image on the right shows the comet IRAS-Araki-Alcock that was discovered with the infrared satellite IRAS. This false-color picture shows its tail at a wavelength of 25 µm (image: NASA/IRAS).

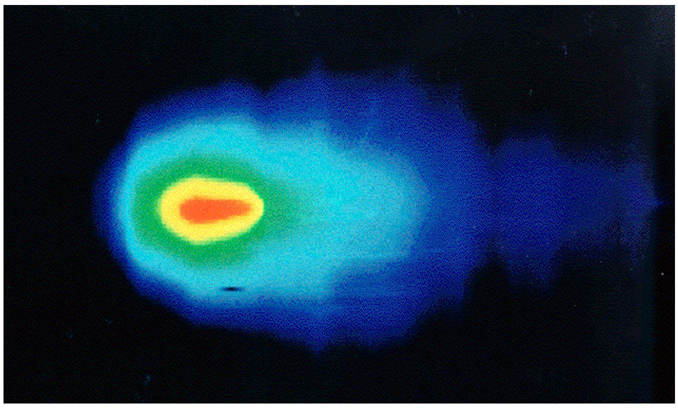

Activity 11: The wooden sphere model of the Earth

With a wooden sphere model, a heat lamp and a thermal IR camera, the absorption and emission of thermal radiation of Earth can be demonstrated. For this purpose, perform three experiments.

Activity 11.a:

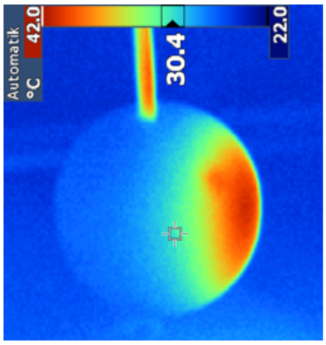

Take the wooden ball and hold it to close the radiating heat lamp for a minute. Then, switch off the light in the room and watch the wooden ball with the thermal IR camera. Describe your observations with regard to the heating of the surface of the sphere.

Activity 11.b:

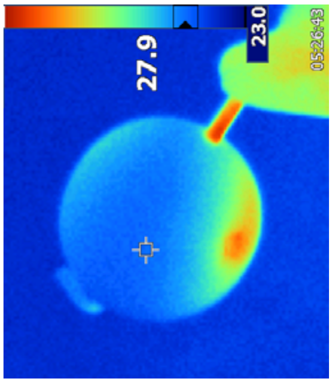

Repeat experiment 11.a after the ball has cooled. This time, rotate the wooden ball slowly around an axis that is perpendicular to the ball-lamp-line. Turn the light off and watch the ball with the thermal IR camera. What has changed compared to the previous experiment?

Activity 11.c:

Repeat the experiment once again, after the ball has cooled. Now, hold it with an inclined axis of rotation at an angle of about 23° compared to the situation before (similar to Earth's axis). One time, the upper part of the ball shows towards the lamp, and the other time, the bottom part of the ball shows towards the lamp. What can you tell this time about each heating surface of the sphere? Compare the wooden ball with the Earth. What facts can be demonstrated?

Activity 11.d:

Find out about the temperatures on the lunar surface. Explain why the temperature differences on the moon are much greater than on Earth. How could this fact be shown with the wooden ball model?

Application in astronomy 5: The puzzle of the atmosphere of planets, or how a disadvantage turns into an advantage

The activities in the chapter 'Barriers to the infrared – absorption in Earth's atmosphere' showed already, that the absorption of infrared radiation is a big disadvantage for ground-based infrared observations.

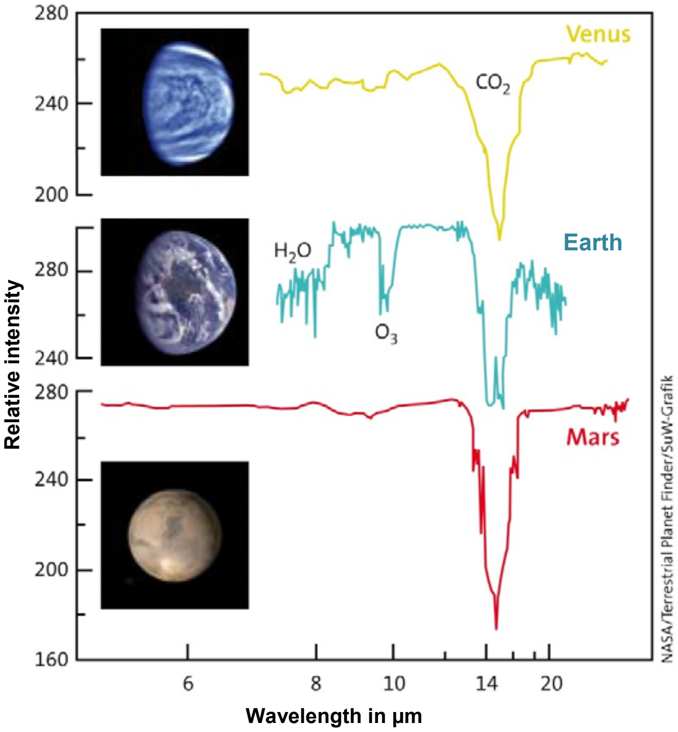

On the other hand, if one would like to characterize the chemical composition of the atmosphere of other planets this is a great advantage. For a long time it remained unclear what chemical substances are in the atmospheres of Venus and Mars. This information was provided by observations in the mid-infrared. The figure on the left shows MIR spectra of Venus, Earth, and Mars. The 'dips' in the graphs are caused by the absorption of MIR radiation by molecules of carbon dioxide, water, and ozone in the planetary atmospheres. Those spectral features are called absorption lines or absorption bands.

The characteristics of infrared absorption are also used to study the composition of planetary rings (e.g. Saturn, Uranus) and tails of comets.

Finding exoplanets using MIR

One of the most interesting fields in modern astronomy is the hunt for exoplanets (extrasolar planets). With the help of various detection methods the existence of 1935 exoplanets have so far been verified (July 27th 2015). The direct approach to finding exoplanets – making an image- has only succeeded a few times. Theoretically it seems more likely to detect exoplanets in the infrared range because the contrast in brightness between star and planet is less at infrared wavelengths (illustration on the right) than at visible wavelengths (illustration on the left; by SuW).

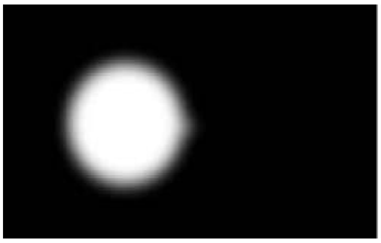

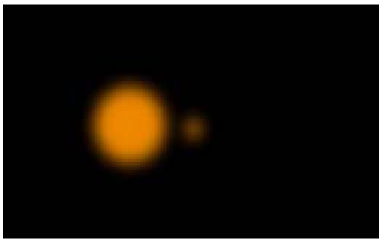

The discovery of exoplanets opens astronomy to interesting connections with chemstry and biology. Ultimately, there is the question whether live exists on other planets, and how one could verify this hypothesis.

The chemical composition of exoplanet atmospheres can be investigated via infrared spectroscopy in the same way that the atmospheres of Venus and Mars were characterized. Researchers are looking for absorption lines and absorption bands, which are like 'fingerprints' of molecules.

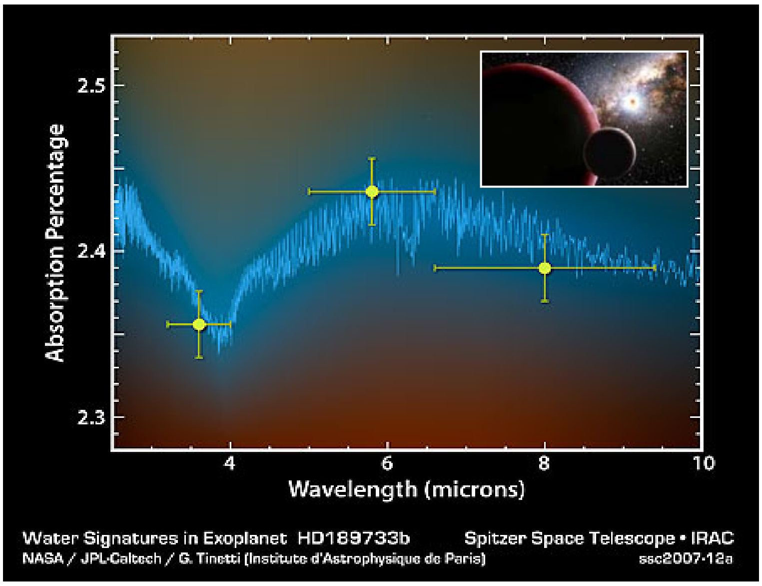

The Spitzer telescope (a space IR telescope) detected water in an exoplanet's atmosphere; however this planet is like the gas giant Jupiter (see figure to the left). If ozone is ever detected in the atmosphere of an exoplanet that could be evidence that life exists on this planet because abundant molecular oxygen can only be produced by living organisms. (image: NASA/Spitzer)

Astronomy in the far-infrared (FIR): emission from objects with very low temperature

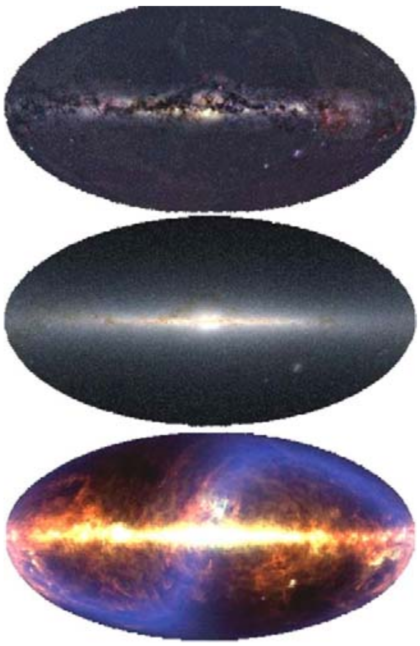

In the FIR almost all stars are invisible, especially if they are located in or around cold dusty areas, because they are hidden in an 'ocean' of FIR-radiation from the cold dust (temperature < 150 Kelvin or about -125 °C). Respectively, we can only see widespread strong emission from the plane of the Milky Way, as shown in the lowest image. The top image shows the galactic disk in visible light; most of the light emitted from the stars is blocked by dust clouds. The middle image shows NIR radiation; at these wavelengths the dust is almost transparent. In the FIR the dust itself is the 'light' source emitting radiation. The FIR image of the galaxy is composed of three images made at wavelengths of 60, 100, and 240 microns by the COBE satellite.

A comparison of an image of Orion in the FIR (on the right) with a picture of Orion at visible wavelengths (left) is really impressive. FIR observations allow the determination of density and distribution of interstellar dust clouds. The strongest emission at 60 microns (symbolized by yellow and white here) is from regions of active star formation.

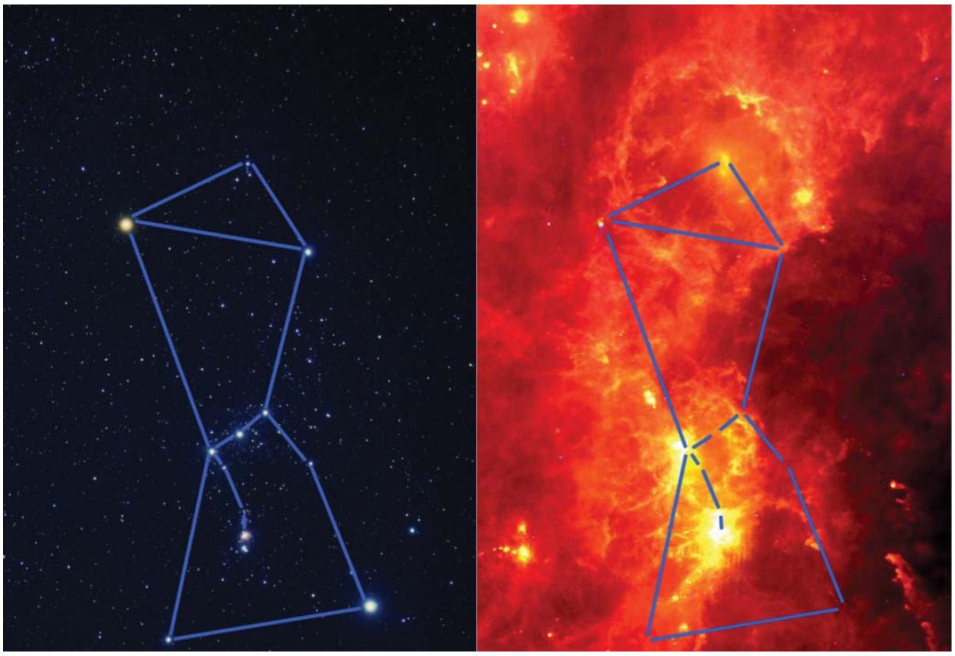

In the table below astronomical objects and the respective temperature are listed and related to different infrared spectral ranges that are used for their investigation.

IR-range	Wavelength (micrometers)	Temperature (Kelvin)	What can be seen?
NIR	0.8 to 5	3000 to 600	Red giants; red dwarfs; stars with circumstellar dust disks; surface of planets, moons, and asteroids; objects in and behind interstellar dust clouds, distant red-shifted galaxies in the early Universe; some molecules
MIR	5 to 30	600 to 150	Thermal radiation from planets, comets and asteroids; heated dust (e.g. protoplanetary material); star forming regions; molecules in planetary atmospheres; molecular clouds (especially biologically important molecules such as H_2O, O_3, CO_2); strongly red-shifted galaxies
FIR	30 to 350	150 to 10	Interstellar (cold) dust; molecules in molecular clouds; early phases in the formation of stars; dust clouds in galaxies with extremely strong emission (e.g. galaxy mergers, starbursts, quasars);
submm	350 to 1000	<10	Cold interiors of dense molecular clouds; first phases of star formation; some molecules

5. SOFIA’s heart – a 15-ton telescope

The German contribution to the SOFIA mission and the heart of the observatory is a 15-ton reflecting telescope built into a 2.5 meter-wide opening in the aft of the fuselage of a Boeing 747SP jet aircraft.

The SOFIA telescope consists of a parabolic primary mirror with a diameter 2.7 m. It is made of Zerodur, a material with a very low thermal expansion coefficient. Silicon carbide is used for the secondary mirror that has a diameter of 35 cm. Its form is convex to elongate the focus. A flat tertiary mirror reflects the radiation through the Nasmyth tube to the scientific instrument that’s connected to the telescope.

It’s an enormous engineering challenge to point a telescope to its target while subject to vibrations of the engines, airflow across the open door, and aircraft maneuvers.

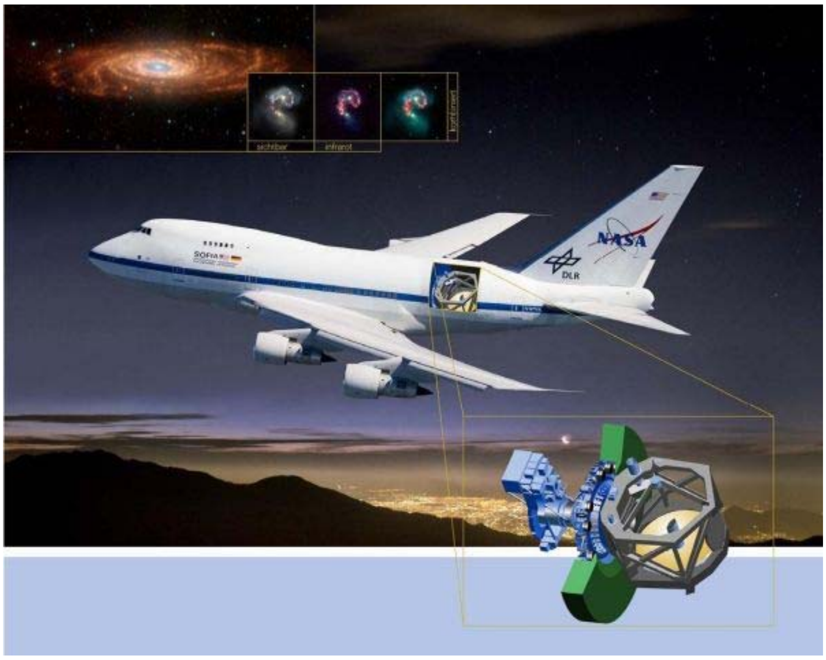

To achieve sufficient stability for astronomy research, the pointing of the telescope must have a precision of 0.2 arcsecond (1 arcsecond = 1°/3600). The following comparison explains the challenge for the engineers: a person on a galloping horse successfully making a sharp image of a 1 cent coin from a distance of 25 km (almost 16 miles).

The telescope door is only opened at full operating altitude. During take-off and landing, and while on the ground, the telescope is protected with the door closed. Between flights, the scientific instrument can be refilled with liquid nitrogen and helium to keep the detectors properly cold.

The flexibility of the aircraft to travel to anywhere around the Earth was successfully used to study the southern hemisphere night sky from New Zealand in 2013 and 2015 and to chase the shadow of Pluto covering a distant star.

Instruments onboard
At the time of this writing (July 2015) researchers can use 7 instruments to observe the universe from SOFIA. These instruments were developed and built in different laboratories in the U.S and Germany. The instruments can be changed, repaired if necessary, updated, and replaced during the planned 20 yearlong observation.

Activity 12: Reflection of thermal radiation

MIR radiation reflects just as visible light does. The following experiment illustrates this. You will need two concave mirrors, which are prepared so that their optical axes lie on a common straight line (for example, using an optical bench). The two concave mirrors each have a radius of r = 19.5 cm, and a peak depth of h = 6 cm.

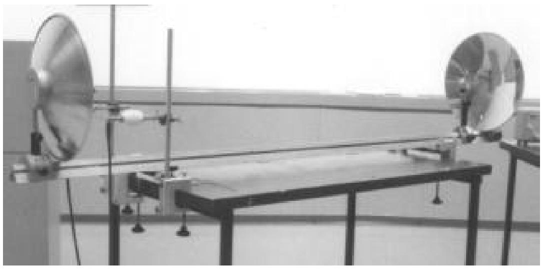

Activity 12.a:

What is the shape of the concave mirror? Is it part of a sphere or is it a type of paraboloid? The result can be determined from the optical axis based on the measurement of a mirror point (x, y) at a distance (x = 5 cm).

Activity 12.b:

Calculate the location of the focal point for the cases that the concave mirror has the shape of a rotation paraboloid or a spheroid. To what degree does the focal length of the concave mirror in these cases differ from each other?

Activity 12.c:

The location of the focal can be determined experimentally. For this reason, a concave mirror can be used with a soldering iron tip in the focal point as a transmitter and a further concave mirror with a thermometer at the focal point as a receiver. Plot the results.

Mathematics and Physics Information Box

Focal length of concave mirrors

Circular paraboloid: $y = a \cdot x^2 \quad \rightarrow \quad f = \frac{1}{4a}$

Spheroid (radius R): $y = -\sqrt{r^2 - x^2} + R \quad \rightarrow \quad f = \frac{R}{2}$

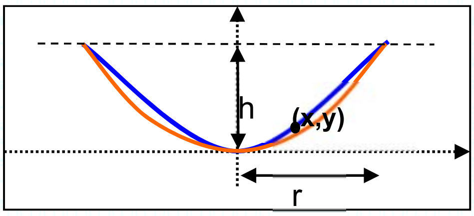

Spherical aberration

To observe extended areas of the sky, telescope mirrors have to be spherical. These kinds of mirrors have spherical aberration, which means light reflected from the inner portion of the mirror has a shorter focal length compared with light reflected from the outer part of the mirror (figure on the left).

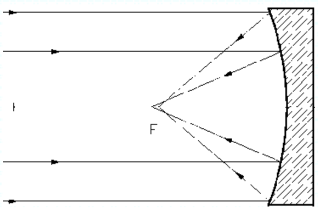

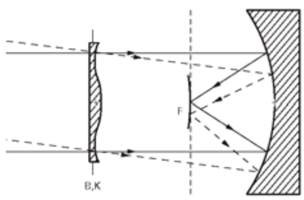

To correct this spherical aberration the optician Bernhard Schmidt developed a corrector plate that is inserted into the light path. It brings light reflected from all parts of the mirror into the same focus, and is called a Schmidt corrector (figure on the right).

Activity 13: Specular and diffuse reflection of MIR radiation

Activity 13.a:

You need a cup filled with hot water (be careful!) a polished metal mirror (without glass), an aluminum plate (which has an oxidized surface), a regular mirror (covered with glass), and a thermal IR camera.


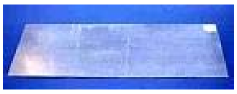

View images of the hot cup reflected from the three different mirrors just using your eye. Now, use the thermal IR camera to look at the reflected images.
Make a sketch from the experiment and describe the results.
Question: Why does the mirror coated with glass reflect the infrared light less well than the one without glass? And why are they both working well at visible wavelengths?

Activity 13.b:

To explain the phenomenon of specular versus diffuse reflection, an analogy can be used. Take a table tennis ball and volleyball and try to understand the differences for both visible and infrared light. Can you design an experiment to investigate this?


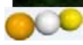

Activity 13.c:

The ability to see details on an object, for example a small scratch, depends on the wavelengths of the light that is used to illuminate it. Lord Rayleigh described the so-called Rayleigh criterion, i.e. the criterion determining the minimum resolvable detail.
Which resolving power α would the human eye have, if the resolving power α is only determined by the size of the aperture (pupil, diameter D = 6 mm)? In reality, what is the resolving power of the human eye and what causes this limit?

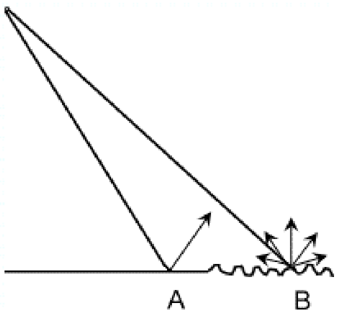

Physics Information Box

If the roughness of the surface is small in comparison with the wavelength of the incident radiation, the reflection is specular, meaning the light ray is reflected at one angle and the surface appears blank (featureless) (case A in the picture).

If the irregularities are bigger than the incident wavelength, the reflection is diffuse, the rays are reflected at different angles and the surface appears rough (case B in the picture).

The extent to which a surface reflects light is defined as the ratio of reflected to incident radiation, termed the ‘albedo.’

Activity 14: SOFIA's vibrations and how they are eliminated

A telescope inside an airplane is an engineering challenge: measures to reduce the vibration must be taken to stabilize the pointing of the telescope. Vibration is caused mainly by the engine and the airflow. To reduce the high frequency vibrations a special synthetic substance is used – a so-called self-damping elastomer. (photograph: NASA/DSI).

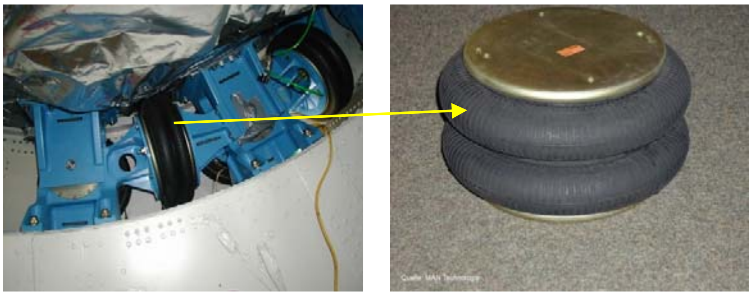

Activity 14.a:

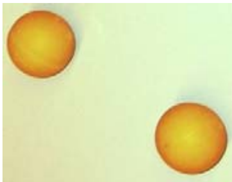

Compare the two rubber balls in regard to their damping ability by letting both balls fall from the same height onto a hard surface. Describe your observations.

Activity 14.b:

The potential energy of 'high-jumping' rubber ball is transformed into kinetic energy. The potential energy of the 'damping' ball is transformed partly into thermal energy. (Potential energy of the starting level → kinetic energy plus thermal energy). Calculate the increase of the temperature if the 'damping' ball is dropped from a height of 2 meters. (Assume ball *mass m* = 20 g, c_{rubber}= 1.4 kJ/(kg·K.)

Activity 14.c: Design an experiment to put mechanical energy into the 'self-damping' rubber ball that shows a remarkable increase of the temperature detectable by the thermal IR camera in comparison with the regular rubber ball.

Astronomy Information Box: Where does the gravitational energy go?

If cosmic objects are getting smaller under the influence of self-gravity or gravitational interaction, thermal energy is released. The energy originates from the free-fall kinetic energy, or if the shrinkage is very slow directly from the potential energy. The temperature of a protostar increases until hydrogen starts burning. The core of a newly-formed planet is hot because of energy released by the collision of millions of planetsimals. A compact stellar remnant can absorb matter from a companion star and collect it into a hot accretion disc that is continual heated by the impact of additional matter. (illustration on the left: http://www.einstein-online.info/spotlights/accretion

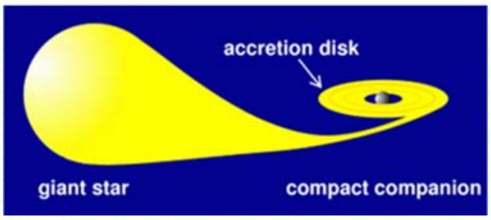

6. Solutions and results for the activities

Activity 1: Perform your own Herschel experiment

Time [min]	Temperature [° C] Blue	Temperature [° C] Green	Temperature [° C] IR
Initial			
1 min			
2 min			
3 min			
4 min			
5 min			

Since the dispersion of prism spectra is not linear (see the related Physics Information Box, 'they stretch towards blue and gather towards red'), the wavelength per unit length in the green region of the spectrum is less than in the infrared region. More radiation energy corresponds to more energy input, i.e. a greater increase in temperature.
Accordingly, the absorption of radiation by the thermometer and its liquid can vary.

Activity 2: The 'Spectrino' – A model for visualizing the electromagnetic spectrum)

Activity 2.a

The radiation of an LED is not due to the temperature of the radiator, as is the case for an incandescent light bulb. Its radiation depends solely on semiconducting properties. While the bulb, which is a so-called thermal source, produces a continuous spectrum, an LED radiates its light in more or less wide spectral bands (spectral ranges).

Top: Views through a hand spectroscope: Continuous light spectrum of a bulb compared to the band spectrum of an LED; bottom: Spectral energy distributions for incandescent light and for LEDs

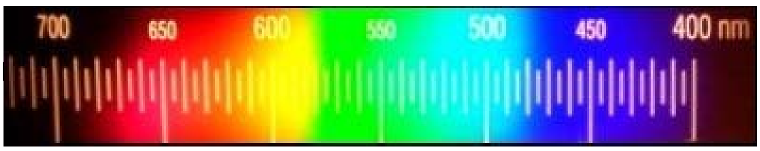

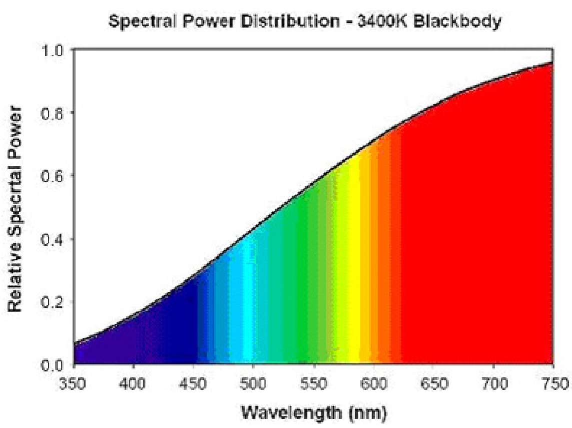

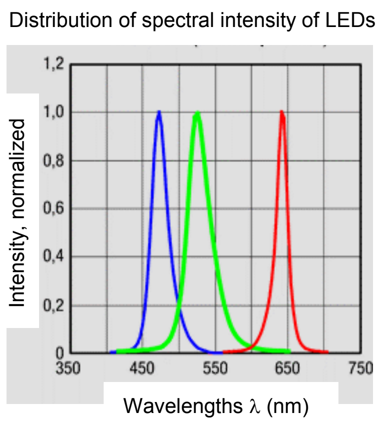

Activity 2.b

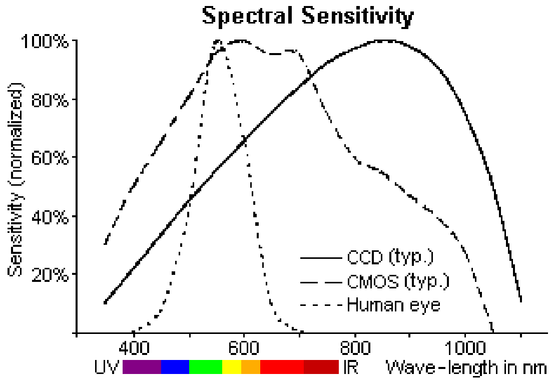

The image sensors of mobile phone cameras (CCD or CMOS) are, in contrast to the human eye, sensitive to NIR radiation and to some extent also to UV radiation (see diagram on the left).

Activity 2.c

- Where does the factor 944 arise from?
  Visible Light: 380 - 750 nm , IR-range: 750 – 350,000 nm

  So: $\dfrac{350,000 \text{ nm} - 750 \text{ nm}}{750 \text{ nm} - 380 \text{ nm}} \approx \underline{\underline{944}}$

- Scale of spectrino: 5 nm → 2mm

  Also: $\dfrac{350,000 \text{ nm} - 750 \text{ nm}}{5 \text{ nm}} \cdot 2 \text{ mm} \approx \underline{\underline{140,000 \text{ mm}}}$

Activity 2.d

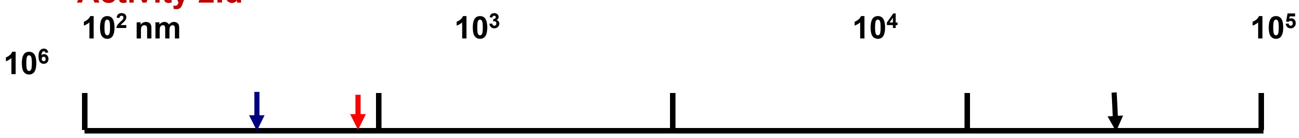

The limits of the spectral range (which are the exponents to base 10 in this scale) can be determined by taking logarithms: e.g. log (380) ≈ 2.6

380 nm ≈ $10^{2,6}$ nm, 750 nm ≈ $10^{2,9}$ nm, 350,000 nm ≈ $10^{5,5}$ nm

Activity 3: The remote control - A near-infrared (NIR) radiator in your living room

Activity 3.a:

Mobile phone cameras are also sensitive to very short-wavelength NIR region (CCD or CMOS photodetector). Therefore, the remote control's or Spectrino's NIR light-emitting diodes can be made visible.

Activity 3.b:

You can change the direction of propagation of the remote control signal just as a visible light beam by reflection or refraction. In order to reflect, an NIR reflecting surface is necessary.

Activity 3.c

The illustrated time axis comprises a time period of approximately 9 ms. Eight pulses are emitted in this period. Thus, in one second, 1000/9 · 8 ≈ 889 pulses are emitted. This corresponds to a frequency of f = 889 Hz. (A young human being can hear sound frequencies from 16 Hz to a maximum of about 20,000 Hz.) This sound is interrupted consistently, when the pulse sequence ends and is retransmitted.

Activity 4: Making NIR radiation audible

Activity 4.a:

Frequencies of electromagnetic radiation visible to the human eye are between $3.8 \cdot 10^{14}$ Hz (750 nm) and $7.9 \cdot 10^{14}$ Hz (380 nm). Sound waves between 16 Hz and 20 kHz are recognized by the (young) human ear.

These two frequency ranges are quite different. (Also note that the physical nature of the two types of waves is completely different.)

Two tones with a frequency ratio between the lower and the higher tone of 1:2 appear quite similar, one octave apart. Hearing is possible over a range of about 10 octaves (16 Hz – 20 kHz).

$16 \cdot 2 \cdot 2 \cdot 2 \cdot 2 \cdot 2 \cdot 2 \cdot 2 \cdot 2 \cdot 2 \cdot 2 \approx 20{,}000$

$16 \cdot 2^x = 20{,}000 \rightarrow x?$

$\log_2(20.000 / 16) \approx \log_2(1250) = \log_{10}(1250) / \log_{10}(2) \approx \log_{10}(1250) / 0.3 \approx \mathbf{10.3}$

In comparison the range for visual perception is within one octave (3.8 : 7.9).

Infrared radiation (about 0.8 – 350 µm), which means frequencies from $3.8 \cdot 10^{14}$ Hz down to about $8.6 \cdot 10^{11}$ Hz, or about **9 octaves.**

$8.6 \cdot 10^{11} \cdot 2 \cdot 2 \cdot 2 \cdot 2 \cdot 2 \cdot 2 \cdot 2 \cdot 2 \cdot 2 \approx 3.8 \cdot 10^{14}$

$\log_2(3.8 \cdot 10^{14} / 8.6 \cdot 10^{11}) \approx \log_2(442) = \log_{10}(442) / \log_{10}(2) \approx \log_{10}(442) / 0.3 \approx \mathbf{8.8}$

Activity 4.b:

The tone corresponding to the frequency of the set of pulses from the remote control corresponds to A440, known as the standard pitch.

Activity 4.c:

sound	**Interval**	**frequency ratio ($f_{note}/f_{keynote}$).**	**Note: color and f**	**Keynote: Color and f**
harmony	Perfect fifth	3:2	Blue ($6.34 \cdot 10^{14}$ Hz => 473 nm)	Red (710 nm => $4.22 \cdot 10^{14}$ Hz)
	Perfect fourth	4:3	Violet blue ($7.03 \cdot 10^{14}$ Hz => 426 nm)	Red (710 nm => $4.22 \cdot 10^{14}$ Hz)
discord	Major seventh	15:8	Dark violet ($7.91 \cdot 10^{14}$ Hz => 379 nm)	Red (710 nm => $4{,}22 \cdot 10^{14}$ Hz)
	Major second	9:8	Red orange ($4.75 \cdot 10^{14}$ Hz => 632 nm)	Red (710 nm => $4{,}22 \cdot 10^{14}$ Hz)

Activity 5: Light emission processes and the energy-level diagram

Activity 5.a:
By comparison of the colors of the emitted light one can conclude that the wavelength is in the green range ($\lambda \sim 550$ nm).
Longer exposure to NIR light leads to a decrease in visible light emitted from the card.

Activity 5.b:

$$E_{550nm} = 2 \cdot E_{NIR}$$
$$h \cdot f_{550nm} = 2 \cdot h \cdot f_{NIR}$$
$$c = \lambda \cdot f \quad \rightarrow \quad f = \frac{c}{\lambda}$$
$$h \cdot \frac{c}{\lambda_{550nm}} = 2 \cdot h \cdot \frac{c}{\lambda_{NIR}}$$
$$\lambda_{NIR} = \lambda_{550nm} \cdot 2$$
$$\lambda_{NIR} = 550 \text{ nm} \cdot 2 = \underline{\underline{1100 \text{ nm}}}.$$

Activity 6: Properties of NIR radiation – Reflection

Plants
Many natural materials reflect NIR radiation quite differently than they do visible light. The diagram shows that the reflectivity of green plants increases in the NIR ($\lambda > 700$ nm). This is caused by the cellular structure of the leaf and the internal water supply system. Both the structure and the supply system are affected in damaged or dying plants. This change leads to a decrease of reflection. The color pigments chlorophyll A and B are especially important for this effect. Their reflectivity changes significantly, and differently, in the range between 400 and 700 nm Therefore, the reflectivity in the IR is an important indicator of a plants health.

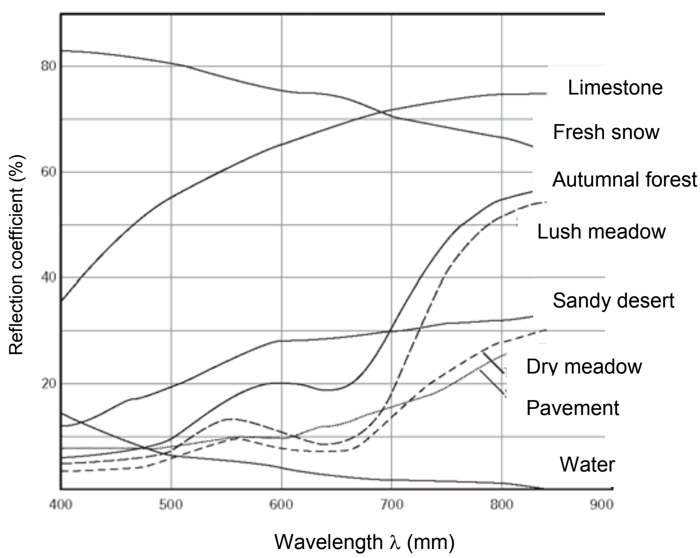

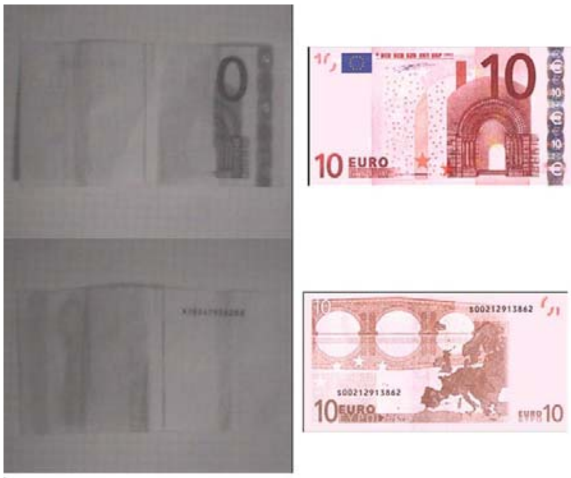

One security feature of paper currency is the ability to reflect NIR radiation. On the front of the 10 Euro bill only one half of the gate and the silver stripe can be seen. At the back of the US 20 Dollar bill a vertical strip of printing on the left side disappears under infrared light.

NIR radiation penetrates deeper into the tissue of the arms so that the veins are visible. The pupil of the eye appears white if a person looks directly into the camera. Typical night-vision surveillance cameras emit NIR radiation to illuminate their surroundings for their NIR-sensitive detector.

Activity 7: Properties of NIR radiation – Transmission and Absorption

In NIR light, Coke is more transparent!

Coke contains caramel color that helps to stabilize the emulsion in sour drinks (like coke). An emulsion is a liquid that contains very tiny droplets of another liquid. In this case, these interact with visible light.

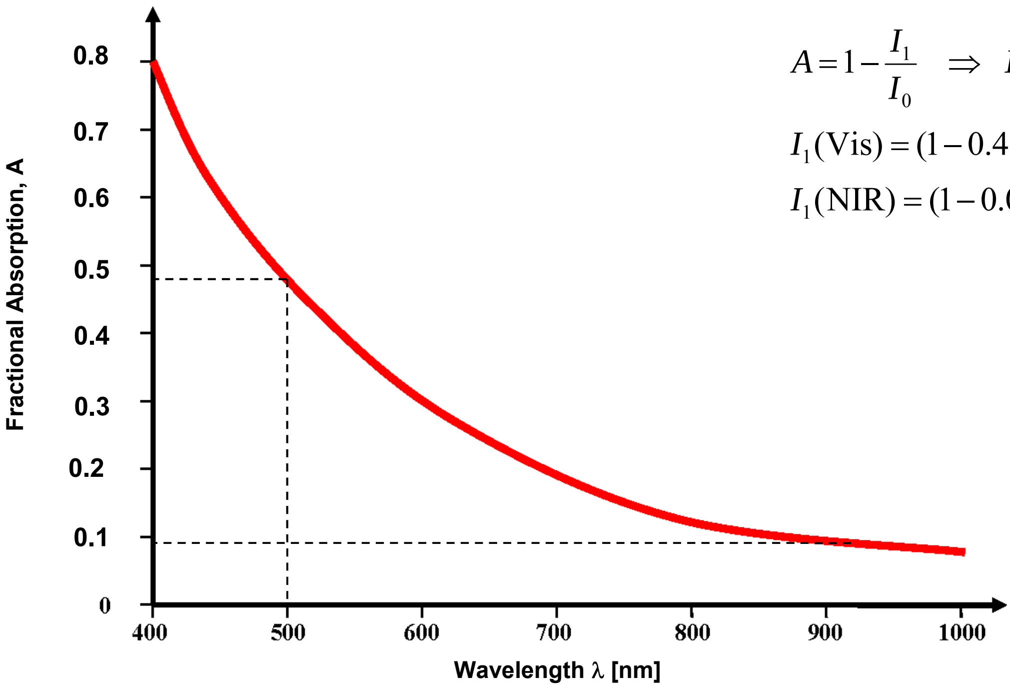

$$A = 1 - \frac{I_1}{I_0} \quad \Rightarrow \quad I_1 = (1 - A) \cdot I_0$$

$$I_1(\mathrm{Vis}) = (1 - 0.48) \cdot 10^6 = 520{,}000.$$

$$I_1(\mathrm{NIR}) = (1 - 0.09) \cdot 10^6 = 910{,}000.$$

Activity 8.b: Coordinate determination with the dark nebula model

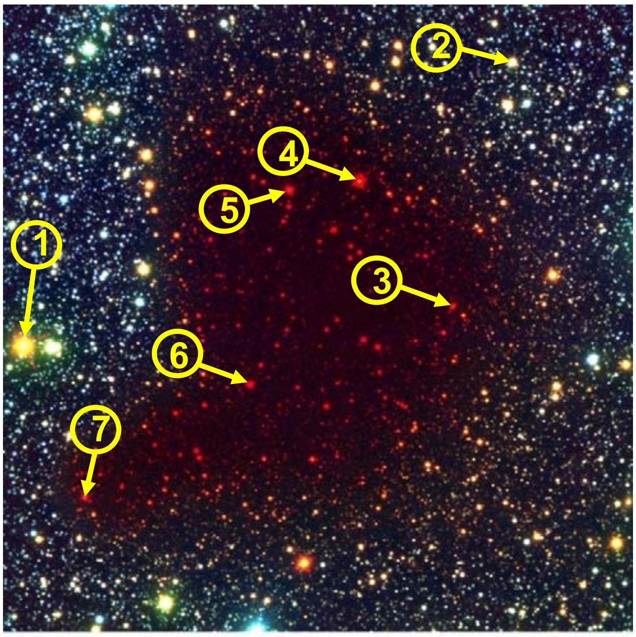

Seeing Through the Pre-Collapse Black Cloud B68
(VLT ANTU + FORS 1 - NTT + SOFI)

ESO PR Photo 02b/01 (10 January 2001)

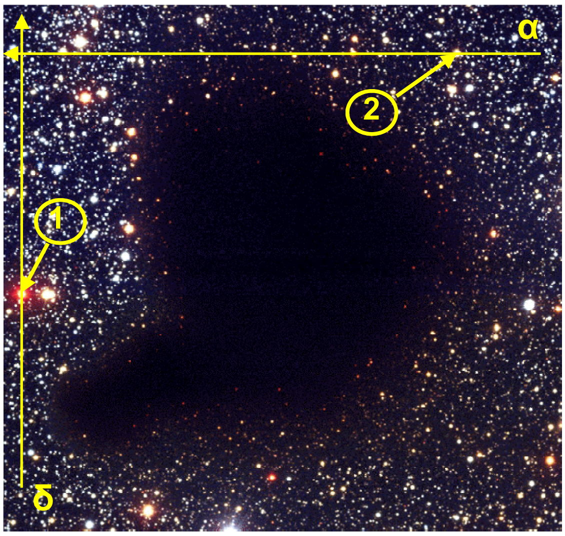

Since each model will vary, one possible solution is described. Here only the very bright stars are used to demonstrate the principle of the activity (see table below). The position of each pixel was determined using the program ‘paint’. The numbers in brackets are absolute positions with regard to the photograph; the other numbers refer to the introduced coordinate system.

Star #	Distance to the reference star 1 in α-direction (mm or pixel)	Distance to the reference star 2 in δ-direction (mm or pixel)	α (h min s)	δ (° ' ")
1	0 (23 pixel)	348 pixel (420 pixel)	$17^h\,23^{min}\,23^s$	-23° 50' 43"
2	596 pixel (619 pixel)	0 (72 pixel)	$17^h\,23^{min}\,6^s$	-23° 48' 31"
3	524 pixel (547 pixel)	299 pixel (371 pixel)	≈-16.9 s $17^h\,23^{min}\,6.1^s$	≈+113" -23° 50' 24"
4	409 pixel (432 pixel)	145 pixel (217 pixel)	≈-13.2 s $17^h\,23^{min}\,9.8^s$	≈+55" -23° 49' 26"
5	324 pixel (347 pixel)	157 pixel (229 pixel)	≈-10.5 s $17^h\,23^{min}\,12.5^s$	≈+60" -23° 49' 31"
6	275 pixel (298 pixel)	395 pixel (467 pixel)	≈-8.9 s $17^h\,23^{min}\,14.1^s$	≈+150" -23° 51' 01"
7	74 pixel (97 pixel)	532 pixel (604 pixel)	≈-2.4 s $17^h\,23^{min}\,20.6^s$	≈+202" -23° 51' 53"

In the α-direction a distance of 596 pixels means a difference $\Delta\alpha$ = 17 s.
1 pixel is therefore 17/526=0.032319 s.
In the δ-direction a distance of 348 pixels means a difference of $\Delta\delta$ =132".
1 pixel is therefore 132/348=0.37931".

Activity 9: Emission of MIR radiation

Activity 9.a:
Eyeglass lenses appear darker because they are cooler than the face, and also the glass absorbs the MIR radiation.

Activity 9.b:
The palm print is visible on the surface of the table because it left a trace of the body warmth. The table surface emits this thermal radiation.

Activity 9.c:
The cold bottle absorbs the warmth of the cheeks, cooling down this area of the face. After the cool bottle is removed less thermal radiation is emitted.

Activity 9.d:
In contrast to visible light, thermal radiation penetrates the black garbage bag or an inflated balloon.

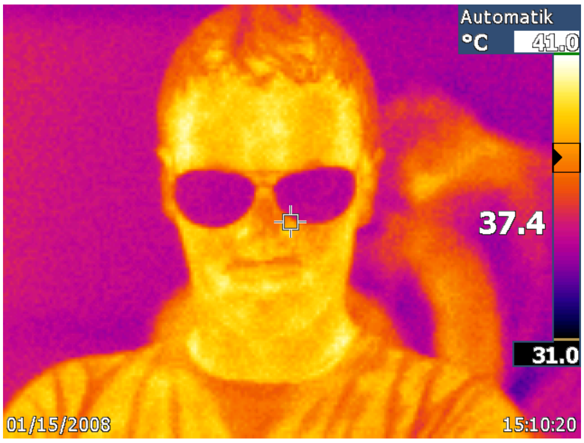

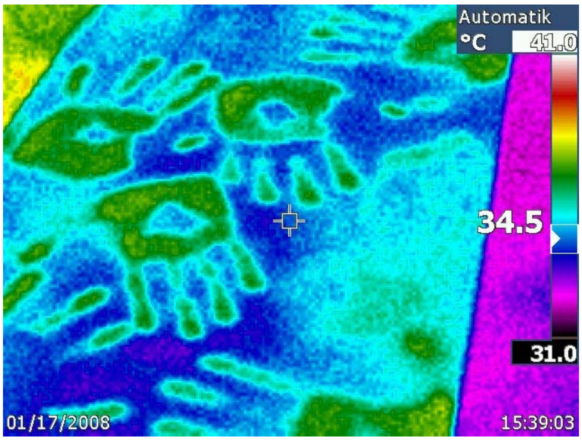

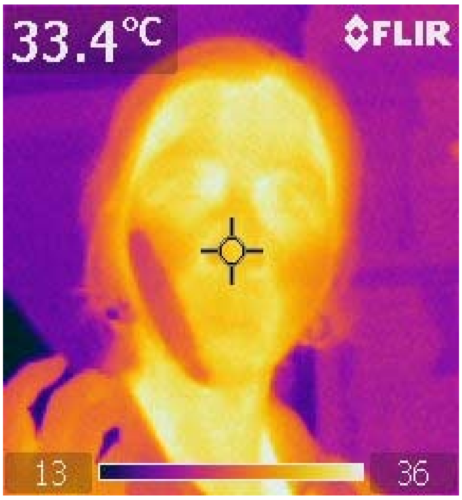

Activity 10: Barriers to the infrared – Absorption in Earth's atmosphere

Activity 10.a:

	air	water
eye (visual)	Radiation visible with no or little reduction (visible)	Radiation visible with no or little reduction (visible)
hand (MIR)	Radiation noticeable with no or little reduction	No radiation noticeable (tangible)


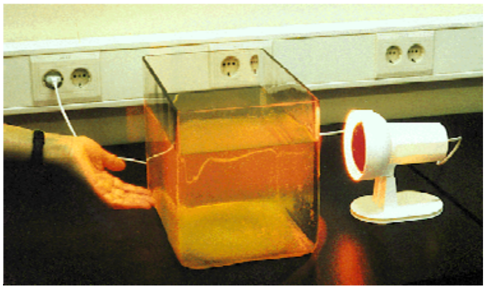


Activity 10.b:

The estimate is based on the following equation:

$$W = m \cdot c \cdot \Delta\vartheta\,.$$

W = amount of heat (kJ)
C = specific heat (kJ/kg K)
M = mass (kg)
$\Delta\vartheta$ = temperature difference between hot and cold side (K)
It's assumed that the temperature is the same in the whole container.

Activity 10.c:

For a harmonic oscillator the period (T) of the oscillation is proportional to the reciprocal of the square root of the spring constant (D).

$$T \sim \frac{1}{\sqrt{D}}$$

	Light wave and water molecule	**Seismic wave and damping element**
NIR	Stretching vibrations	Spring with high spring constant D (hard spring)
MIR	Bending vibration	Spring with medium spring constant D (medium spring)
FIR	Rotational vibration / rotation	Spring with a low spring constant D (soft spring)

Activity 11: The wooden sphere model of Earth

Activity 11.a:

A circular area of the wooden sphere model is heated. The intensity of the heating depends on the angle of incidence of the radiation. The strongest warming is in the area of the sphere's 'equator'.

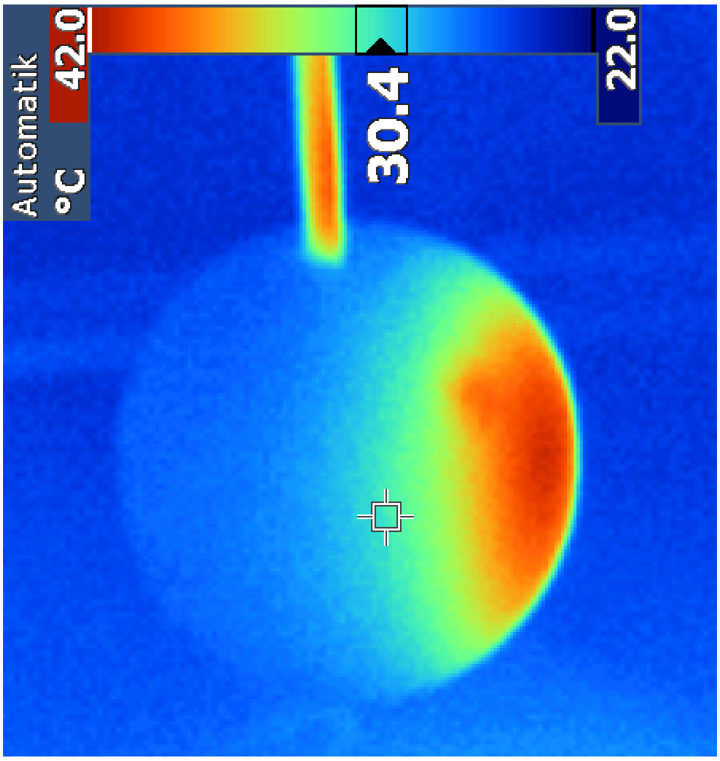

Activity 11.b:

The warming is detectable around the whole sphere along the equator. The warmest area is the spot with the most recent exposure to radiation.

Activity 11.c:

This time the heated area isn't along the equator but is tilted by the angle through which the axis of the sphere is inclined. The seasons of the year are explained the same way.

Activity 11.d:

The temperature on the surface of the moon is 130°C on the side towards the Sun and –160 °C on the far side. Unlike Earth, the Moon doesn't have an atmosphere, and also the rotation of the Moon is very slow (about 27 days per rotation). The rapid cooling of the side opposite the Sun can readily be shown by rotating the wooden sphere slowly while observing it with the thermal IR camera. The effects of an atmosphere could be replicated by wrapping the sphere in plastic foil.

Activity 12: Reflection of thermal radiation

Activity 12.a:

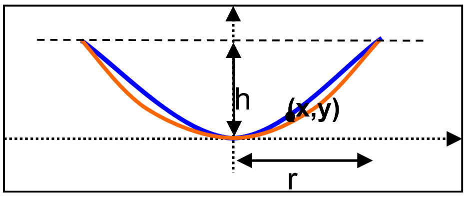

At a distance of x = 5 cm from the optical axis the distance of y can be calculated of for a **paraboloid:**

$$y = 6\,\text{cm} - a \cdot x^2 = 6\,\text{cm} - \frac{0.01578}{\text{cm}} \cdot 5^2\ \text{cm}^2 \approx 5.6\,\text{cm}.$$

At a distance of x = 5 cm from the optical axis the distance of y can be calculated for a **spheroid:**

$$y = 6\ \text{cm} - \left(-\sqrt{r^2 - x^2} + R\right) = 6\ \text{cm} - \left(-\sqrt{34.7^2\text{cm} \ -5^2\ \text{cm}} \ +34.7\ \text{cm}\right) \approx 6.4\ \text{cm}.$$

Activity 12.b:

In case of a **paraboloid**:

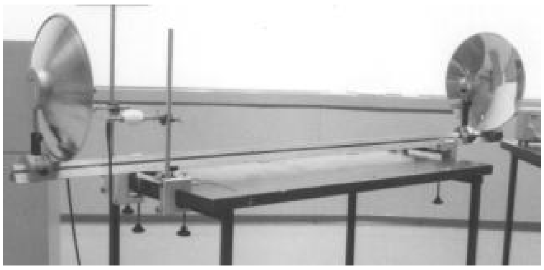

$$y = a \cdot x^2 \quad \Rightarrow \quad a = \frac{y}{x^2} = \frac{6\,\text{cm}}{19.5^2\,\text{cm}^2} \approx \frac{0.01578}{\text{cm}}.$$

The focal point is $\frac{1}{4a} \approx 15.8\,\text{cm}.$

In case of a **spheroid:**

$$y = -\sqrt{r^2 - x^2} + R \quad \Rightarrow \quad R = \frac{y^2 + x^2}{2y} = \frac{(6\,\text{cm})^2 + (19.5\,\text{cm})^2}{2 \cdot 6\,\text{cm}} \approx 34.7\,\text{cm}.$$

The focal point is about 17.3 cm.
The difference between both focal points is about 1.5 cm.

Activity 12.c:

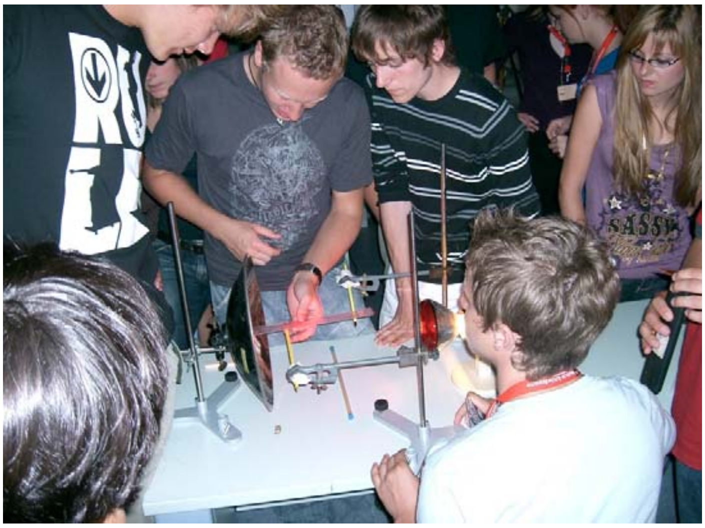

The photograph shows the measurement of the focal point for NIR radiation. The focal point was determined using a thermometer that was – step by step – moved along the optical axis.

Activity 13: Specular and diffuse reflection of MIR radiation

Activity 13.a:

The matte aluminum plate reflects MIR radiation very well, due to the relatively long wavelength and the rough surface that doesn't diffuse the radiation. On the other hand, the rough surface diffuses rays with shorter wavelengths such as visible light – the aluminum plate has a diffuse reflection at shorter wavelengths. The normal, glass coated mirror reflects visible light, but part of the MIR is absorbed by the glass.

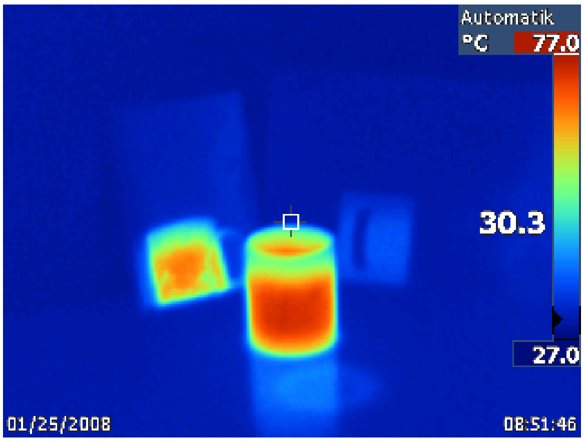

Activity 13.b:

With the following analogies the interaction of different wavelengths with different surfaces can be explained. If you drop a volleyball on washed-out concrete (a little rough) it bounces back precisely – analogous to specular reflection. If you drop a table tennis ball instead, it will bounce back in an unpredictable direction – analogous to diffuse reflection. The volleyball corresponds to the MIR case and the tennis ball to the visible light case.

Activity 13.c: The resolving capacity of the human eye

To calculate the resolving capacity of the human eye the Rayleigh criterion is used:

$$\alpha = 1.22 \cdot \frac{\lambda}{D} \quad (\alpha \text{ in radians})$$

$$\alpha = 1.22 \cdot \frac{0.55 \cdot 10^{-6}\ \text{m}}{0.006\ \text{m}} \approx 1.12 \cdot 10^{-4} \quad \rightarrow \quad \alpha^{\circ} \approx 0.0064° \approx 23''.$$

The resolving capacity of the human eye is about 2' (2 arcminutes). It is actually limited by the density of photoreceptor cells in the retina.

Activity 14: SOFIA's vibrations and how they are eliminated

Activity 14.a:

The normal rubber ball bounces off the floor (elastic impact) almost back to the height it was dropped. Only a little part of the kinetic energy is lost.

The rubber ball consisting of the self-extinguishing elastomer bounces only a little (inelastic impact). The kinetic energy is mostly transformed into heat (energy). In real applications it is important to calculate the expected heating of damping elements. If the stress on the material is too high, it can be destroyed.

Activity 14.b:

The mass of the ball isn't important if we hypothesize that the whole mechanical energy of the impact is transformed into thermal energy:

$$m \cdot g \cdot h = m \cdot c_{rubber} \cdot \Delta T$$

$$\Delta T = \frac{g \cdot h}{c_{rubber}} = \frac{9.81\,\mathrm{m} \cdot 2\,\mathrm{m} \cdot \mathrm{g} \cdot \mathrm{K}}{\mathrm{s}^2 \cdot 1.4\,\mathrm{J}} = \frac{9.81\,\mathrm{m} \cdot 2\,\mathrm{m} \cdot \mathrm{g} \cdot \mathrm{K}}{\mathrm{s}^2 \cdot 1400\,\frac{\mathrm{g} \cdot \mathrm{m}^2}{\mathrm{s}^2}} = \underline{\underline{0.014\,\mathrm{K}}}.$$

Activity 14.c:

One possibility is to put each ball in a net with a 1 m line and hit the nets including the balls onto the floor 50 times – at the same time and with the same impact. Immediately observe the balls with the thermal camera.

7. Literature about SOFIA

SOFIA oder warum die Astronomen in die Luft gehen, Krabbe, A., Titz, R., Röser, H-P, Sterne und Weltraum, 12/1999, S.1052

Das SOFIA-Projekt -- neue Perspektiven für Forschung und Bildung, Fischer, O., Titz, R., in Astronomie+Raumfahrt im Unterricht 5/1999, S. 37

Deutsches SOFIA Institut gegründet, Althaus, T., Sterne und Weltraum, 4/2005, S. 14

Astronomie in luftigen Höhen, Scorza, C., 2008, Sterne und Weltraum, 7/2008, S.

SOFIA – Die Sternwarte über den Wolken, Scorza, C., in Astronomie und Raumfahrt im Unterricht, 10/2009, S.15

Information about SOFIA: https://www.sofia.usra.edu/
https://www.dsi.uni-stuttgart.de/

<u>online Versions:</u>
German version:
http://www.dsi.uni-stuttgart.de/bildungsprogramm/lehrmaterial/ir-strahlung/Handbuch-IR-
English version:
http://www.dsi.uni-stuttgart.de/bildungsprogramm/lehrmaterial/ir-strahlung/Manual-IR-Kit.pdf

<u>Contact:</u>

Dr. Antje Lischke-Weis
Educational and Public Outreach
Deutsches SOFIA Institut
Stuttgart
Germany
lischke@dsi.uni-stuttgart.de
phone + 49 711 68562130